The thesis committee for Francisco Javier Gonzalez-Castillo
certifies that this is the approved version of the following thesis:

Characterization of PolyJet Additive Manufacturing in Support of
Model-Based Definition

APPROVED BY
SUPERVISING COMMITTEE:

Carolyn Seepersad, Supervisor

Richard Crawford

Characterization of PolyJet Additive Manufacturing

in Support of Model-Based Definition

by

Francisco Javier Gonzalez-Castillo

Thesis

Presented to the Faculty of the Graduate School

of The University of Texas at Austin

in Partial Fulfillment

of the Requirements

for the Degree of

Master of Science in Engineering

The University of Texas at Austin

May 2023

Characterization of PolyJet Additive Manufacturing

in Support of Model-Based Definition

by

Francisco Javier Gonzalez-Castillo, MSE

The University of Texas at Austin, 2023

Supervisor: Carolyn Seepersad

The versatility, precision, and ability to create complex geometries afforded by Additive Manufacturing (AM) make it a valuable tool for product designers, engineers, and manufacturers. While AM offers several advantages, the lack of recognized product definition and design standards is a significant barrier to widespread adoption. Product definition practices like Model-Based Definition (MBD) make forming a standardized hub for information about an AM process easier.

PolyJet manufacturing, an AM process, has various materials and unique capabilities and would benefit significantly from MBD. To enable the use of MBD, Design for AM (DfAM) guidelines for PolyJet must be formed for communicating design intent and manufacturing requirements. Great strides have been made in forming DfAM guidelines for PolyJet. However, no comprehensive metrology studies have been done to characterize the multi-material printing capabilities unique to PolyJet.

Three metrology test parts are designed to characterize the PolyJet process and its post-processes. Parts #1 and #2 evaluate the performance of single-material vs. multi-material parts,

feature resolution, and geometric accuracy. Test part #3 characterizes the survivability of features in the post-processing stage. All parts are evaluated across different feature sizes and build orientations for a robust understanding of the PolyJet process. The results are compiled into graphs, color-coded charts, and data analysis that guide future designers to avoid unnecessary re-design and part failure.

Table of Contents

List of Tables

List of Figures

Chapter 1: Introduction

1.1 Motivation

Additive Manufacturing (AM) is the process in which products are created by building up material layer by layer. AM has afforded product designers new design tools that enable them to create products with complex features that are infeasible with traditional manufacturing. Its versatility, precision, and ability to create complex geometries make it a valuable tool for product designers, engineers, and manufacturers. However, the unique nature of AM also makes current product definition and design communication frameworks impractical. For instance, researchers at the University of Minnesota used CT scans to create anatomical models of their patients' hearts to evaluate their candidacy for surgical procedures using AM, as shown in Figure 1 [1]. The intricacies of the anatomic models' fabrication make it challenging to capture enough product information for other medical professionals to replicate the parts using engineering drawings alone.

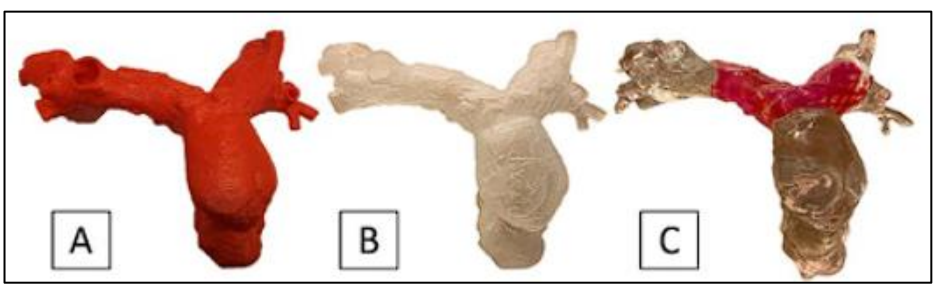

Figure 1: AM printed models of the patient's arterial system for candidacy examinations. Image: [2]

AM products often employ various materials, finishing techniques, and design rules across the different AM processes, making it compelling for researchers to consider how to communicate all the details of AM products and processes moving forward. Traditionally, two-dimensional drawings capture product information, as seen in Figure 2, and serve as the source of "truth."

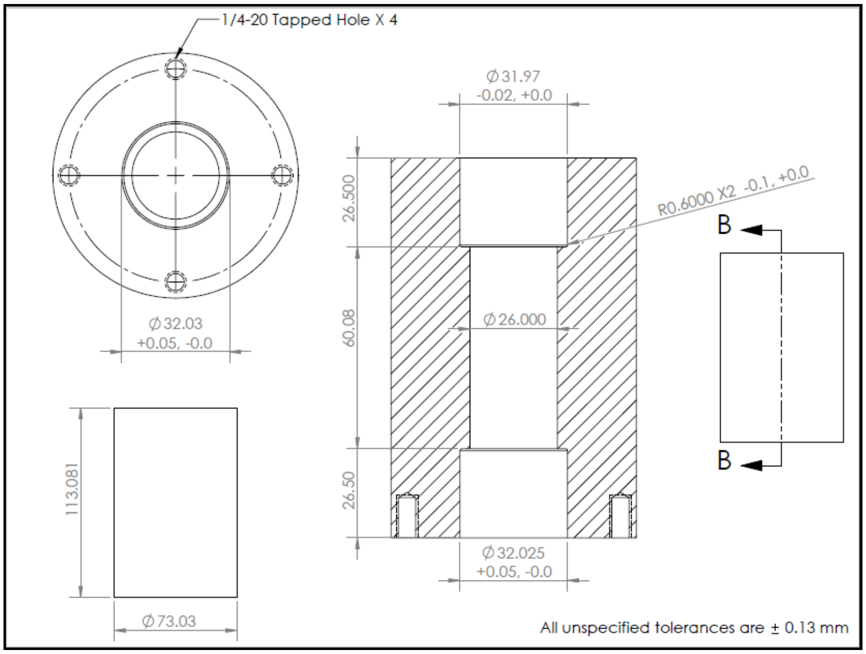

Figure 2: Traditional 2-Dimensional shop drawing for a generic cylindrical housing

These conventional approaches in product definition are difficult to transfer to products made with AM processes because AM product definition is not standardized. Standardization is a critical component of the manufacturing industry because it is an agreement between manufacturers to follow guidelines and constantly pushes them to improve their processes and products. The lack of recognized standards for AM products, processes, and materials is one of the biggest challenges to the widespread adoption of AM technology [3]. Emerging practices like Model-based Definition (MBD) can address this challenge by offering an innovative approach to standardizing AM product definition.

MBD is a digital process for defining and communicating product and manufacturing information. MBD is a data-driven approach that uses 3D models as the primary source of product information, eliminating the need for traditional 2D engineering drawings. Figure 3 showcases a 3-D model with product annotations that define its geometric information. MBD's dynamic and detailed product representation makes it well-suited to convey the complex geometries and process-specific information associated with AM products [4].

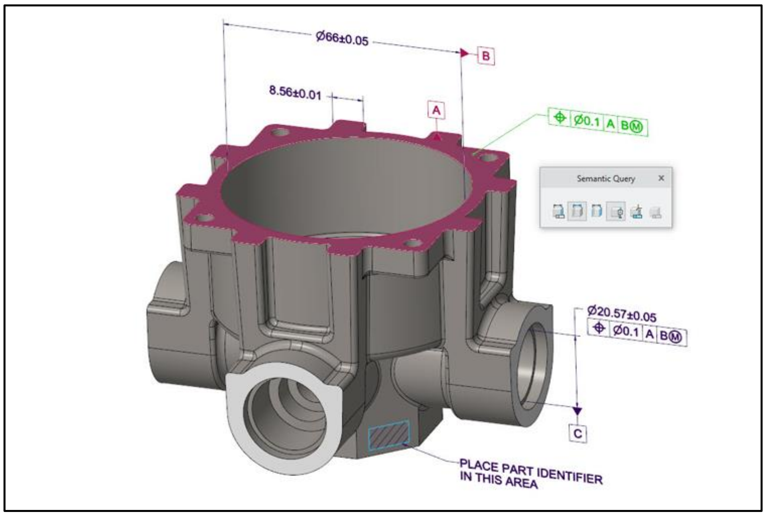

Figure 3: MBD product containing geometric product dimensions and application information that can be interacted with to view all product surfaces. (Image: [5])

In MBD, the 3-D model serves as a digital hub for manufacturing information which streamlines the communication of product and manufacturing information (PMI) in the product life cycle stages. A study conducted by the National Institute of Standards and Technology (NIST) found that the use of MBD reduced the time required for the design annotation, manufacture, and inspection cycle by up to 74.8% over traditional 2-D drawings because of the high level of detail and reduced ambiguity afforded by the technical data package (TDP) of products made with MBD [6]. A TDP is a compilation of files containing varying product definition documentation such as standard GD&T, alternative product images, manufacturing, application, and inspection information.

Organizations like the DoD and ASME have already published several standards to bolster the widespread use of MBD practices. Standards like *MIL-STD-31000A* formalize the contents of a TDP, including the different product views, copyright information, application information, and any other information the user deems necessary for comprehensive product definition, as shown in Figure 4.

State Name	Description of Contents Displayed
• 0_Model_Only	Although it is not required for MBD this view is recommended to quickly hide all annotation displaying only the model
• MBD0_Default	Legal notice, Proprietary notice, ITAR notice and/or other company specific notices. NOTE**:** File to be saved in this state
• MBD1_Site_Map	Notes identifying all available combination views – 3D roadmap
• MBD2_Titles	Title Block information (Company name, design description, model number, cage code, design signatures, block tolerances, material and finish requirements)
• MBD3_Properties	Overall boundary dimensions, mass properties, material, finish requirements and title block information
• MBD3_Characteristics	Optional – Key characteristics
• MBD4_Notes	General note information
• MBD5_Set_Datums	Set datums
• MBD6_User_Derfined	Exploded Views and Assembly Unique views
• MBD7_User_Defined	Define the details of the Machining operations using annotations
• MBD8_User_Defined	Define the details of the Welding operations using annotations

Figure 4: General content guidance from MIL-STD-31000A for each section of an MBD technical data package. [29]

Similarly, *ASME Y12.14-2019* offers insight into applying traditional GD&T annotations to "digital products" to guide those transitioning from using 2-D drawings to defining products with MBD in mind. In addition to the developments in MBD for traditional products, implementing MBD practices for Additive Manufacturing (AM) processes is an emerging subset of MBD research.

The most current work in the field is ASME-Y14.46-2022 and ISO/ASTM 52900-15, which introduce standard practices for defining terminology, products, and technologies unique to AM. For example, ASME Y14.46 provides guidance for defining infill geometries and lattice structures unique to AM, as shown in Figure 5. The combination of pushing the MBD envelope in terms of standards and defining AM-specific characteristics further underlines the suitability of MBD to serve as the principal method for defining AM products.

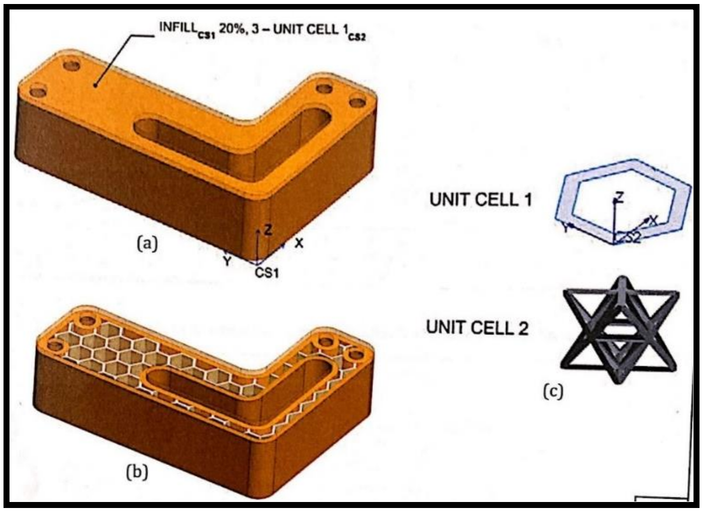

Figure 5: Recommended Practice for defining different bounded volume regions distinguish the varying unit cell patterns in the internal lattice structure. (Image: ASME Y14.46, Figure 4-28)

Although there have been great strides in formalizing AM product definition, creating a set of guidelines that applies to all processes is challenging. All AM processes have unique capabilities, limitations, and opportunities, making it critical to study each process and create designer guidelines to improve the process of fabricating AM parts. Metrology studies can bridge this understanding gap and allow designers to use advanced product definition techniques like MBD to make the AM part life cycle more efficient. Metrology allows researchers to develop detailed and statistical knowledge about a particular process by evaluating the geometric performance of printed parts. Many researchers have used metrology benchmark parts to reliably characterize how a machine resolves certain features such as holes, unsupported overhangs, surface roughness, and overall geometric accuracy to obtain information on AM process limitations [7] [8].

Characterizing AM processes allows designers to generate designs that align with a process/machine's capabilities and limitations to ensure no issues when manufacturing. The context in which designers operate for an AM process is known as a Design for Additive Manufacturing (DfAM) framework. The objective of a DfAM framework is for designers to maximize product performance subject to the capabilities of the underlying AM technology [9]. DfAM research is extensive and spans multiple areas of AM and AM processes, but there is still work to do in generating design rules from experimental methods [10]. Processes like PolyJet, which can produce complex parts with multiple materials, are well-suited for metrology studies and characterization but are often not prioritized in DfAM research compared to other processes, such as fused deposition modeling and powder bed fusion [11].

1.2 PolyJet and DfAM

AM processes such as PolyJet, which has a wide variety of materials and unique capabilities, would benefit significantly from using product definition practices like MBD and having a DfAM framework in place. PolyJet is a subset of material jetting technology that uses multiple printer heads to deposit thin layers of liquid photopolymer resins, typically between 16 and 32 microns thick, and then cures the layer with UV lamps until the part is fully formed. The PolyJet process (Figure 6) offers a wide range of capabilities because it can use multiple print heads that deposit materials of different rigidities and colors.

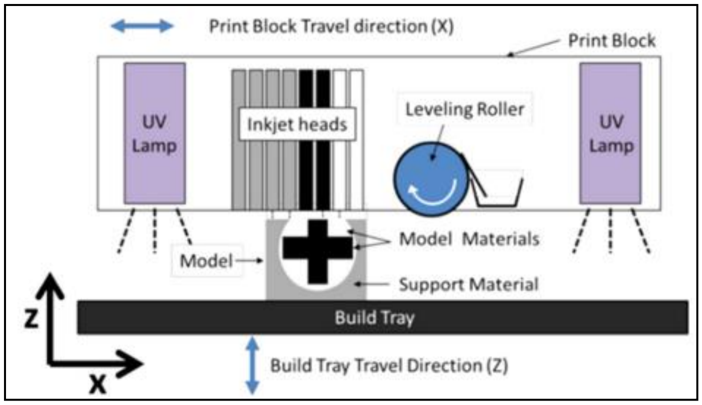

Figure 6: PolyJet process overview schematic (Image [8])

The ability to print multiple materials simultaneously can be leveraged to form parts with various material properties, colors, designs, and overall part complexity. The part shown in Figure 7 uses materials of different stiffnesses and colors to simulate the intramuscular structure of a hand, which is only possible with the PolyJet process.

Figure 7: Anatomical model of a human hand built with PolyJet (Image: Medprint.com)

The great detail and complexity of parts created with PolyJet have motivated several researchers to characterize aspects of its parts, such as the mechanical properties of materials [12], geometric accuracy [13], and surface roughness [14]. However, many of these studies aim only to characterize a single PolyJet process parameter, pertaining to a specific application, and do not evaluate the multi-material capabilities of PolyJet [8]. This lack of characterization makes a detailed metrology study paramount to developing a DfAM framework that designers can reference.

1.3 Research Goals

This thesis presents metrology studies on the PolyJet process using benchmark test parts to characterize PolyJet and its post-processes. The results from the benchmark tests presented can be used to create a detailed set of DfAM guidelines for the PolyJet process. DfAM guidelines serve as a way for researchers and designers working with the PolyJet process to navigate the design space more effectively and create a basis for the standardization of the process.

Another goal is to contribute to the landscape of AM standardization and the widespread adoption of MBD for AM. The DfAM guidelines from the metrology studies create a basis for outlining a comprehensive product definition schema for products made with the PolyJet process in future work.

Chapter 2: Previous Work

2.1 Benchmark Parts

Metrology is the scientific study of measurement and can be very broad in application. For AM research, metrology serves as quality control for AM processes [15]. One can collect qualitative and quantitative data about an AM process's performance using metrology tools such as benchmark test parts. A benchmark part is a test specimen that allows researchers to measure the performance of an AM process and parts. Benchmark parts typically fall into one of the following three categories: 1) process benchmarks, 2) mechanical benchmarks, and 3) geometric benchmarks [16]. A process benchmark (Figure 8-A) is a test artifact to establish the optimal process-specific parameters for maximizing a characteristic like geometric accuracy or build speed. Mechanical benchmarks (Figure 8-B) evaluate the mechanical properties of the parts and materials from an AM process. Geometric benchmarks (Figure 8-C) highlight a process or machine's performance in resolving geometric features or a specific design capability. The work presented in this thesis primarily employs geometric benchmarks to characterize the unique design capabilities afforded by PolyJet.

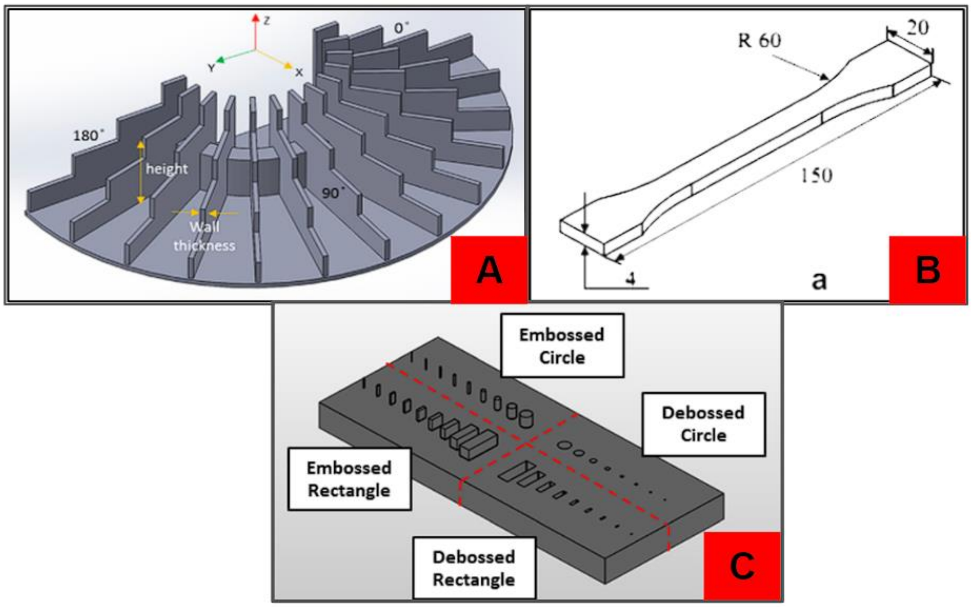

Figure 8: A) Process benchmark for evaluating optimal build orientation when resolving vertical walls with the PolyJet process [13], B) Mechanical benchmark tensile bar for finding tensile strength of fused deposition modeling materials [17]. C) Geometric benchmark for determining PolyJet's ability to resolve small embossed/debossed features [8].

2.2 Minimum Feature Size

Characterization of PolyJet via benchmark parts is a growing subset of metrology research. Many researchers seek to characterize the PolyJet process in support of a specific goal or project. For example, Braian et al. [18] conducted a study evaluating the ability of different AM processes, including PolyJet, to accurately print dental benchmark parts. Meisel et al. [8] conducted a study using several benchmark parts to characterize the capability of PolyJet to resolve unsupported overhangs, debossed holes/slots, and embossed holes/slots (Figure 8-C). In their study, they printed several test parts that were post-processed and evaluated for their geometric fidelity with a digital microscope. The researchers tested these parts for the two surface finish options offered by the PolyJet process. The researchers also examined the capability of the PolyJet process to resolve unsupported overhanging features, as shown in Figure 9.

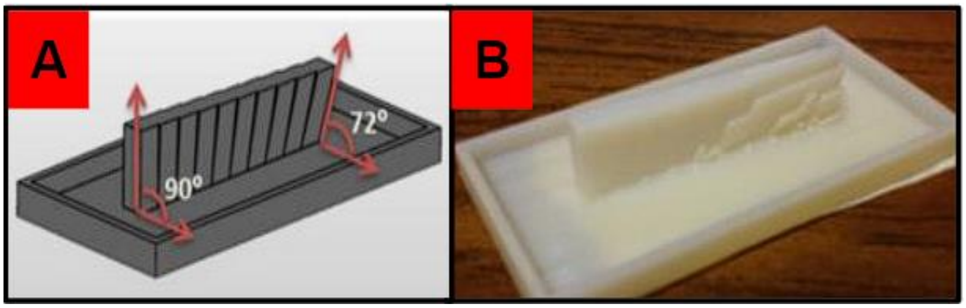

Figure 9: A) Test part for self-supporting angle with an angle gradient from 90-72 degrees, B) Test part after printing showing where the overhanging features cannot resolve (~85 degrees from the build plate). Image: [8]

This study was extensive in its characterization of the PolyJet process using various benchmark parts. However, the study did not include any metrology aimed at characterizing the multi-material capabilities afforded by PolyJet. The multi-material capabilities should be prioritized in the characterization of PolyJet since they are unique to the process. Tee et al. [19] conducted a study where their goal was to characterize the mechanical properties of multi-material parts and their geometric resolution. Figure 10 demonstrates some of the test specimens used in the study, which evaluated the minimum resolvable composite features using Agilus30 (elastomeric) and VeroMagentaV (rigid). The study highlights some key characteristics of the multi-material capabilities when printing composite features. However, the study was limited since it did not evaluate the composite feature resolution across layers or compare their performance to non-composite features with the same process parameters.

Characterizing composite features in different orientations and comparing them to the non-composite features is critical to understanding process capabilities and the effects of composite features on resolution and accuracy. The work presented in this thesis aims to fill this gap in knowledge regarding composite features and those with uniform material to provide a complete examination of the performance of the PolyJet process and its unique capabilities.

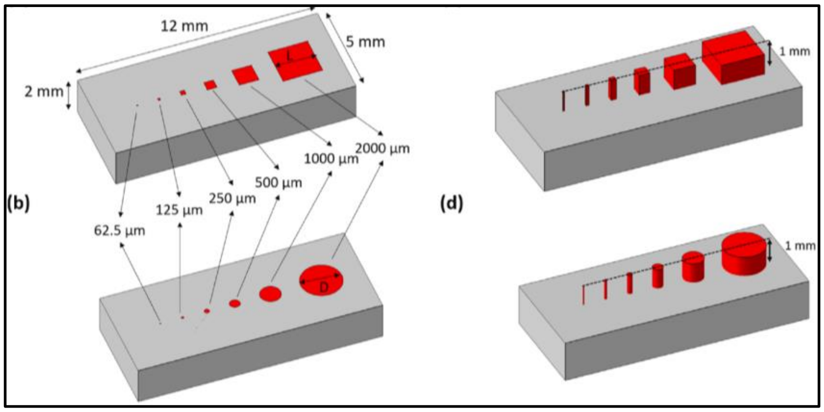

Figure 10: Benchmark part used to evaluate minimum feature size of composite geometric features. Image: [19]

2.3 Geometric Accuracy Characterization

Many researchers primarily focus on the geometric accuracy of AM processes in their metrology studies. These studies evaluate the effects of different build parameters, such as build orientation [20], layer thickness [21], material [22], and surface finish [13]. Researchers use various measurement tools like coordinate measuring machines (CMM), calipers, optical scanners, and digital micrometers to evaluate the dimensional accuracy of printed parts, with CMM being the most commonly used due to its high fidelity. One paper reviewed 37 geometric accuracy studies for PolyJet and found that process parameters such as smaller layer thickness, glossy surface finish, and Vero White material led to greater dimensional accuracy, among other process parameters [23]. However, several of these results were only consistent across three studies or less. The process parameter evaluated the most in the review, build orientation, was the most inconsistent across 8 studies. These results indicate that metrology studies must be tailored to the process, part, or machine being characterized. The work presented in this thesis aims to provide comprehensive guidelines for the PolyJet process in general, along with a benchmark test part that can be used to characterize a specific PolyJet machine.

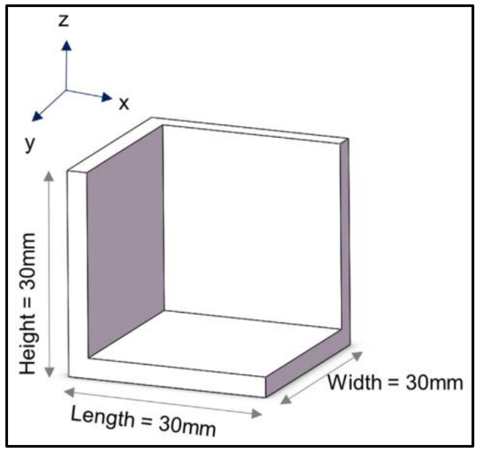

Figure 11: Process benchmark part designed to evaluate the geometric accuracy of the PolyJet process. This part was measured in all three axes (XYZ) to determine which axis yields the most accurate geometry. Image: [13]

2.4 Post-Process Characterization

After fabrication, PolyJet parts must also undergo post-processing which can be a limiting factor when resolving small features. The standard support cleaning process for PolyJet parts uses a high-pressure water jet and alkaline solution to remove supports from printed parts. This procedure can be harsh and negatively affect the survival of features post-processing. Research on the characterization of the post-process associated with PolyJet is limited and usually consists of general guidelines from online forums and videos. Miesel et al. [8] evaluated the efficiency of the standard support removal techniques and the "survivability" characteristics for PolyJet parts shown in Figure 12.

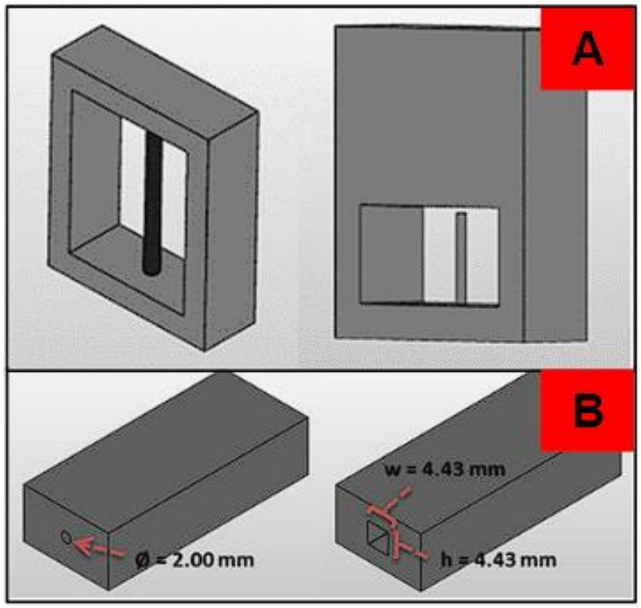

Figure 12: A) The test specimen has small columns to determine survivability after post-processing, B) Test specimens with long, support-filled channels are post-processed to evaluate the effectiveness of the water jet on different geometries. Image: [8]

In their study, researchers tested the survivability of columns with various configurations in their fixture (cantilevered vs. fixed on both ends), material (elastomeric vs. rigid), shape (rectangular vs. circular), and cross-sectional area. The results showed that a specimen's cross-sectional area limits support removal techniques' efficiency for support-filled channels, and the diameter of the survivability features had the most impact, with rigid columns having a limit of 1.13 mm and elastomeric at 3.0 mm. This study was very comprehensive and unique, as there is not a wide range of literature on the post-processing of PolyJet parts. However, the researchers did not incorporate the manufacturer-recommended alkaline solution in their post-processing. For PolyJet, SUP706 is the most commonly used support material. Stratasys, the company that produces SUP706, recommends hands-free removal with a 2% solution of sodium hydroxide and sodium metasilicate or mechanical removal by hand or waterjet [24]. The alkaline solution and additional attachments for the waterjet cleaning station can drastically improve the survivability of features and contribute to the characterization of PolyJet post-processes.

Overall, ample room exists for additional characterization of PolyJet and its post-processes. The work presented in this thesis aims to fill some of these gaps in metrology and provide a benchmark part and a set of design guidelines that support product definition practices associated with post-processing of PolyJet. Design allowables for multi-material printing, build orientation, and support removal are all critical areas of interest for this thesis.

Chapter 3: Part & Experimental Design

3.1 Introduction

To successfully perform a metrology study and characterize PolyJet, a test part must be designed with measurable features. Although other PolyJet test parts have been proposed in the literature, there must be a new test part that addresses the three primary gaps identified in the literature for characterizing PolyJet:

- **Minimum Resolvable Features**
  - Multi-material geometric features in different orientations,
  - Single-material geometric features in different orientations.
- **Geometric Accuracy**
  - Multi-material vs. single-material features,
  - Effects of build orientation on geometric accuracy.
- **Survivability**
  - Effects of different support removal techniques and build orientation.

To address these gaps, three metrology parts were created for gathering and analyzing data from the PolyJet process. Part #1, shown in Figure 13, is a single-material metrology part that characterizes debossed features' geometric accuracy and minimum resolvable size. Similarly, part # 2 has the same geometry as part #1 but with secondary material inlays instead of voids, as shown in Figure 14. These two parts characterize how well multi-material features resolve compared to uniform-material features. Additionally, if a geometric feature resolves before post-processing, there must be an evaluation of whether a feature survives post-processing. Part #3, shown in Figure 15, highlights the survivability characteristics of small features in post-processing and the effectiveness of two post-processing techniques.

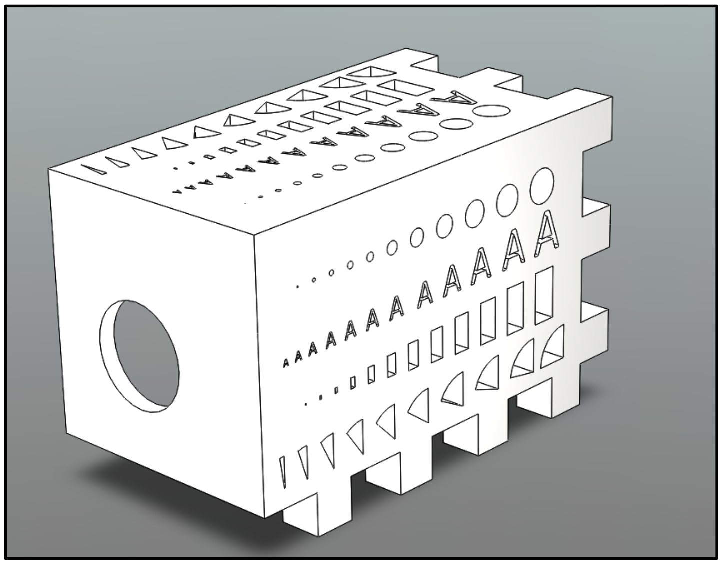

Figure 13: Test part #1 evaluates PolyJet's capability to print a variety of debossed geometric features to evaluate the minimum resolvable features and geometric accuracy.

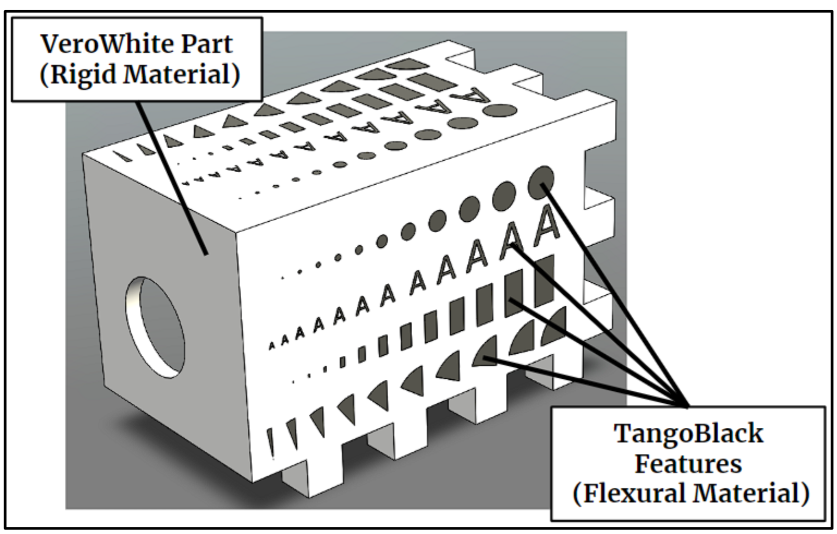

Figure 14: Test part #2 evaluates PolyJet's capability to print a variety of multi-material geometric features to evaluate the minimum resolvable features and geometric accuracy.

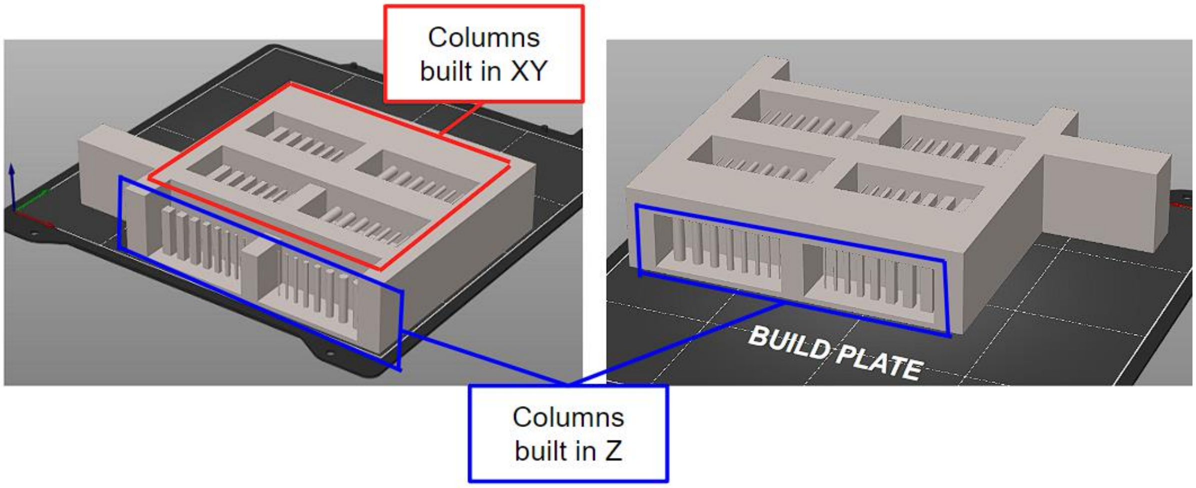

Figure 15:Test Part #3 evaluates the effect of build orientation on the survivability of geometric features. There are four sets of column features for each build orientation (Z and XY)

3.2 Single-material and Multi-material Parts

The complete list of features and their specifications for parts #1 and #2 are presented in Table 1. All features were fabricated on two different faces of each test part: the top face and a side face as shown in Figures 13 and 14.

Table 1: Specifications of all geometric features in test Part #1 and their descriptions.

Features	Range	Description
Circles	Diameter: 4 mm - 0.2 mm	Eleven circular features with the following diameters: 4, 3.5, 3, 2.5, 2, 1.5, 1, 0.8, 0.6, 0.4, 0.2.
Slots	Length: 6 mm - 0.2 mm Width: 3mm - 0.1mm	Twelve slots with a ratio of 2:1 for length to width. Each subsequent rectangle has a decrement of 0.6 mm in length and 0.3 mm in width
Text	Font: 18 pt - 3 pt	Twelve text features in Calibri font with the following point sizes:18,16,14,12,10,9,8,7,6,5,4,3.
Angles	Angles: 90 – 9 degrees	Ten quarter-circles with a radius of 4 mm that decrement by 9 degrees in each instance.

Part #1 characterizes the minimum resolvable features for various single-material features. The size range across the different geometric features was determined using the dimensions of those in similar studies. Feature sizes are determined so that the larger features are expected to resolve while smaller features are expected to fail. This highlights the cut-off in feature resolution, which serves as a design guideline for designers.

In addition to resolving general geometric shapes, it is critical to characterize feature characteristics such as angled faces. As the angle between two adjacent surfaces decreases, so does the gap between them. Yap et al. [13] performed a study in which they found that when the gap between two surfaces is too small, agglomerates form between surfaces and cause them to fuse. Similarly, part #1 aims to characterize the same effect with small, angled faces.

Multi-material features customize a part's aesthetics or mechanical properties by depositing multiple materials simultaneously and curing them. Similar to the study by Tee et al. [19], where researchers printed multi-material test parts with circular and rectangular features, part #2 was designed to characterize how well PolyJet can resolve sharp corners, curved edges, and geometric features unique to PolyJet, such as embedded text.

A multi-material part is a 3D assembly of all components with assigned materials. For example, to have a block with a circle of a different material, the circular feature and the surrounding structure must be assembled and assigned their respective material, as shown in Figure 16.

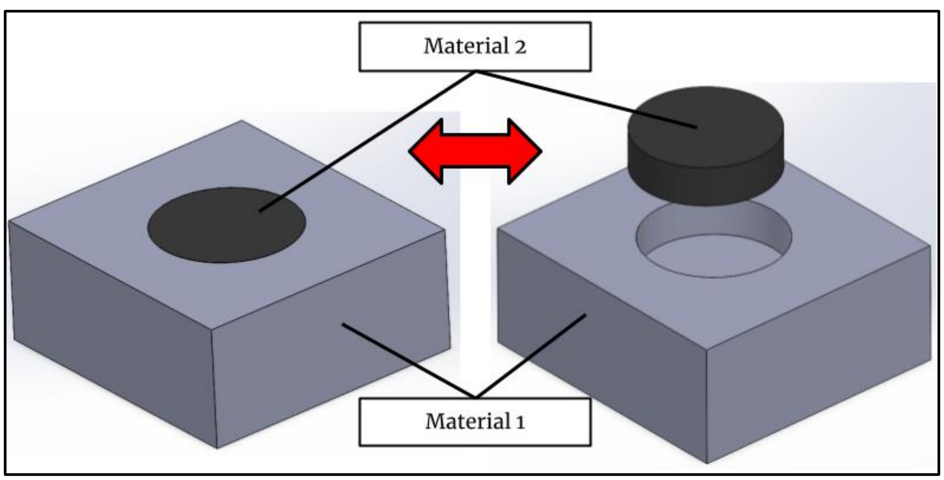

Figure 16:The schematic highlights how multi-material features are created in the model by assembling the components of different materials for printing on PolyJet.

One of the applications for the multi-material functionality is to embed text in the surface of the part using dissimilar materials, so text was printed on Part #2 in different font sizes to characterize the ability to embed text or graphics into the printed part using multiple contrasting materials.

3.3 Material Selection

When selecting the materials for the multi-material test parts, employing two contrasting materials presents an extreme case for multi-material features. A stark contrast between the two materials makes it easier to observe the resolution of the multi-material features. It is also helpful to select common materials to make the results applicable to a broader audience of designers. VeroWhite and TangoBlack meet the criteria for materials as they contrast in color and mechanical properties. VeroWhite is a rigid white material that is part of the "Vero" family of materials offered by Stratasys and is widely used by large companies for prototyping. TangoBlack is a black flexural material that contrasts with VeroWhite. Both materials are readily available at various AM retailers, so they were selected for the metrology parts.

3.4 Build Orientation

The build orientation of a geometric feature relative to material layers significantly affects the identified problem areas. Features built with their cross-sections orthogonal to the build plate, known as inter-layer features, are resolved in the Z-direction, as shown in Figure 17. Features built with their cross-sections parallel to the build plate, known as intra-layer features, are resolved in the XY plane. For example, the features in Figure 17 highlight two adjacent surfaces on part #1 that represent the two different build orientations being evaluated.

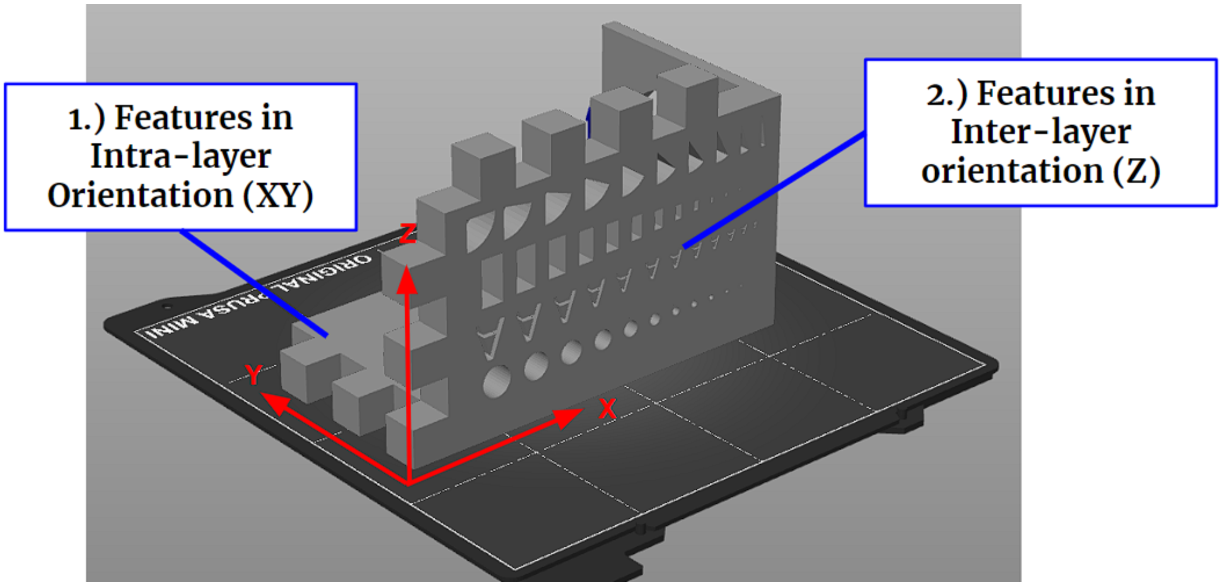

Figure 17: The two faces of parts #1 and #2 contain the same geometric features. Each face is intended to characterize a build orientation.

The Stratasys J750 offers a high resolution of 600 dpi on the X-axis, 300 dpi in the Y-axis, and 14-27 microns in the Z-axis [25]. The difference in resolution between the two orientations makes it critical to characterize how geometric features are affected by the build orientation.

3.5 Support Removal

Post-processing PolyJet parts is a critical stage in the production process. Supports are typically removed using a high-pressure waterjet cleaning station with a pressure of approximately 1750 psi. This pressure can damage small or delicate features in post-processing. Fortunately, supports can be removed by soaking parts in an alkaline solution. As supports are almost unavoidable when printing PolyJet parts, identifying the best practice for post-processing is critical to understanding the PolyJet process. The work presented in this thesis uses benchmark parts and various support removal techniques to determine the best post-processing practices for maximizing feature survivability.

When preparing a model for printing, the Stratasys J750 offers two surface finish options: matte and glossy finish. The glossy finish avoids using support material for the part when possible, and the matte surface finish encapsulates the entire geometry in the support material. Figure 18 illustrates how these different surface finishes appear.

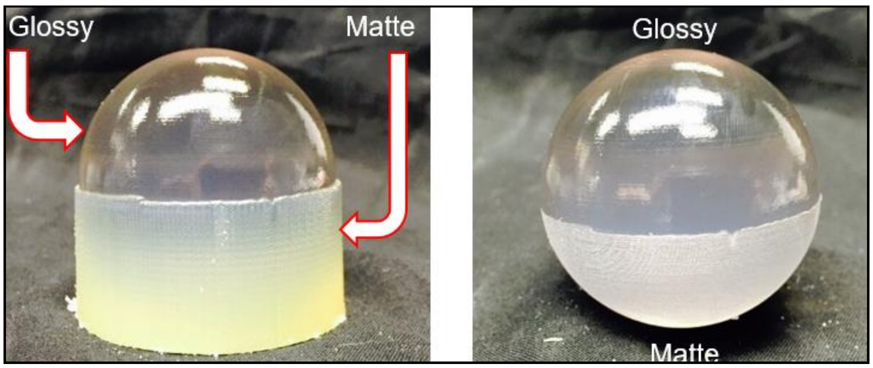

Figure 18: This spherical geometry on the left is printed with a glossy surface finish, but due to the nature of the lower hemisphere, support material was necessary to resolve the feature, resulting in a matte finish. (Image: grabcad.com)

Previous work characterizing the best practices for post-processing PolyJet parts is minimal. Most notably, Meisel et al. [8] performed experiments to determine the suitable dimensions for small features to survive the support removal process. In their experiments, researchers cleaned small column features with different support connectivity (cantilever vs. fixed), cross-sectional shape (rectangular vs. circular), and material (rigid vs. flexural) with a high-pressure water jet and observed how many successfully survived. However, in their study, the researchers neglected to address how the build orientation of the columns affects their survivability. As previously mentioned, build orientation can significantly impact the performance of a part and its mechanical properties. Test Part #3 has column features like the ones in the previous study to address the gap in knowledge of how build orientation affects the survivability of geometric features. Test Part #3 includes eight sets of columns to evaluate how survivability varies across different column fixtures, build orientation, cross-sectional shape, and size combinations. Figures 19 - 20 and Table 2 highlight how each set of columns is specified in test Part #3.

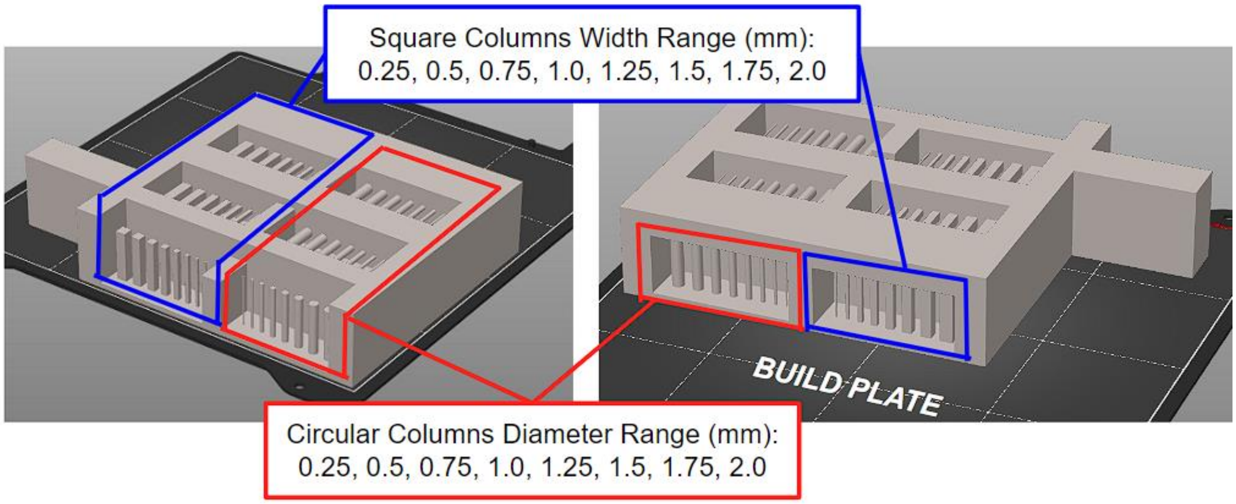

Figure 19: Dimension ranges for columns in Part #3 and their shape.

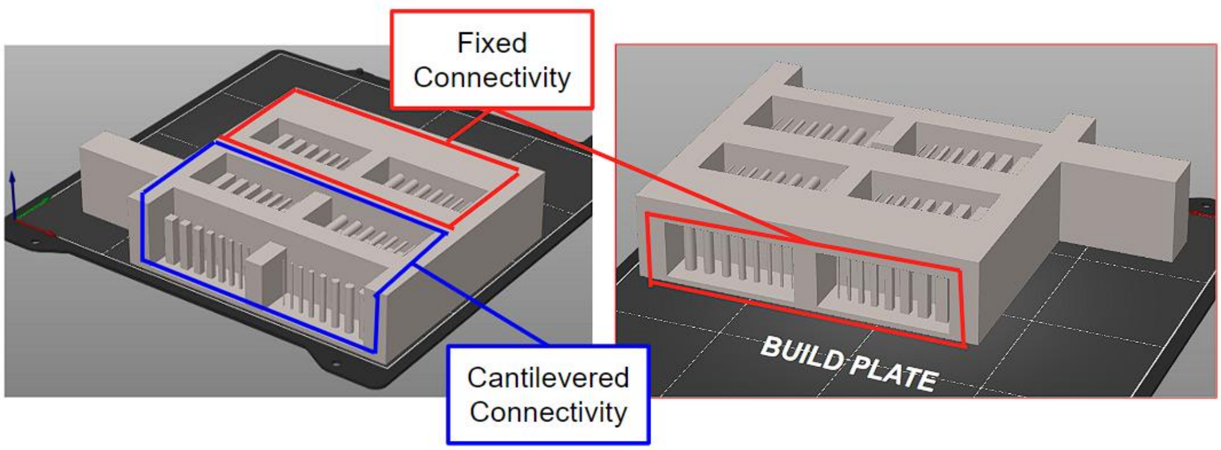

Figure 20: Part #3 feature connectivity of columns.

Table 2: Description of features in part #3; each section has two sets of columns, one in the ZY (across layers) build orientation and one in the YZ (along layers) build orientation.

Section 1	Circle, cantilevered columns
Section 2	Square, cantilevered columns

Section 3	Circle, fixed columns
Section 4	Square, fixed columns
Column Width/ Diameter (mm)	2, 1.75, 1.5, 1.25, 1.0, 0.75, 0.5, 0.25

For the presented work, only the matte surface finish is considered because having all surfaces coated in support material can be regarded as a "worst case" for testing support removal techniques. Additionally, two support removal techniques are compared to determine how to maximize the survivability of geometric features. For the first technique, a two-minute water jet stream that concentrates the pressure on a small area (Figure 21- A) is applied. In the second technique, a conical water stream that distributes the water pressure across the part surface (Figure 21- B) is applied for two minutes, and then the part is soaked in an alkaline solution for 60 minutes.

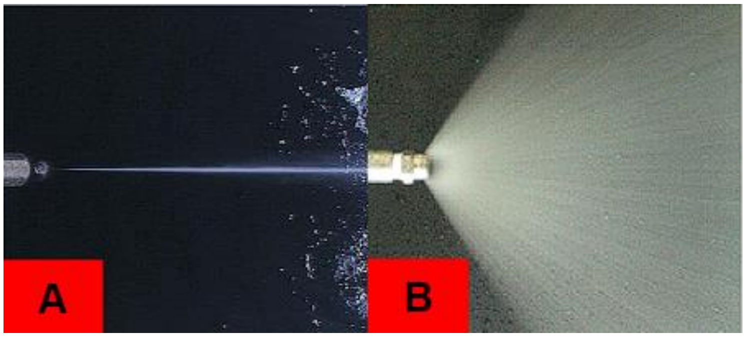

Figure 21: Two different water jet cleaning techniques used to determine how to improve the survivability of small geometric features undergoing post-processing. (Images: kirinoikeuchi.co.jp)

To ensure sufficient data to rule out any outliers when evaluating the survivability of the various features, a total of eight parts were printed, four for each cleaning technique. Table 3 shows how data is collected for the geometric features and support removal techniques associated with test Part #3.

Table 3: Survivability table for test Part #3 is organized to include connectivity, cross-sectional shape, build orientation, cleaning procedure, and feature size.

Conical Tip								
Fixed Connectivity								
	0.25	0.5	0.75	1.0	1.25	1.5	1.75	2.0
Square ZY								
Square YZ								
Round ZY								
Round YZ								
Cantilevered Connectivity								
	0.25	0.5	0.75	1.0	1.25	1.5	1.75	2.0
Square ZY								
Square YZ								
Round ZY								
Round YZ								

Water Jet								
Fixed Connectivity								
	0.25	0.5	0.75	1.0	1.25	1.5	1.75	2.0
Square ZY								
Square YZ								
Round ZY								
Round YZ								
Cantilevered Connectivity								
	0.25	0.5	0.75	1.0	1.25	1.5	1.75	2.0
Square ZY								
Square YZ								
Round ZY								
Round YZ								

3.6 Geometric Accuracy

There are many methods for gathering geometric accuracy data from physical parts, with the CMM being among the most prominent. The CMM uses physical probes to quantify the dimensions of the physical part relative to the CAD model. However, multi-material features do not have notable physical borders or edges for a CMM to measure, so images from an *AM Scope* stereo microscope were used to measure the geometric accuracy. The microscope is calibrated with a millimeter standard, allowing the built-in software to relate the number of pixels to physical distances.

Additionally, small tabs are included on the outer edges of test parts #1 and #2 to measure the overall part accuracy in the X, Y, and Z axes with the CMM. Figure 22 shows the design features for measuring the geometric accuracy of parts #1 and #2, including a hole for fixturing the test part onto the CMM.

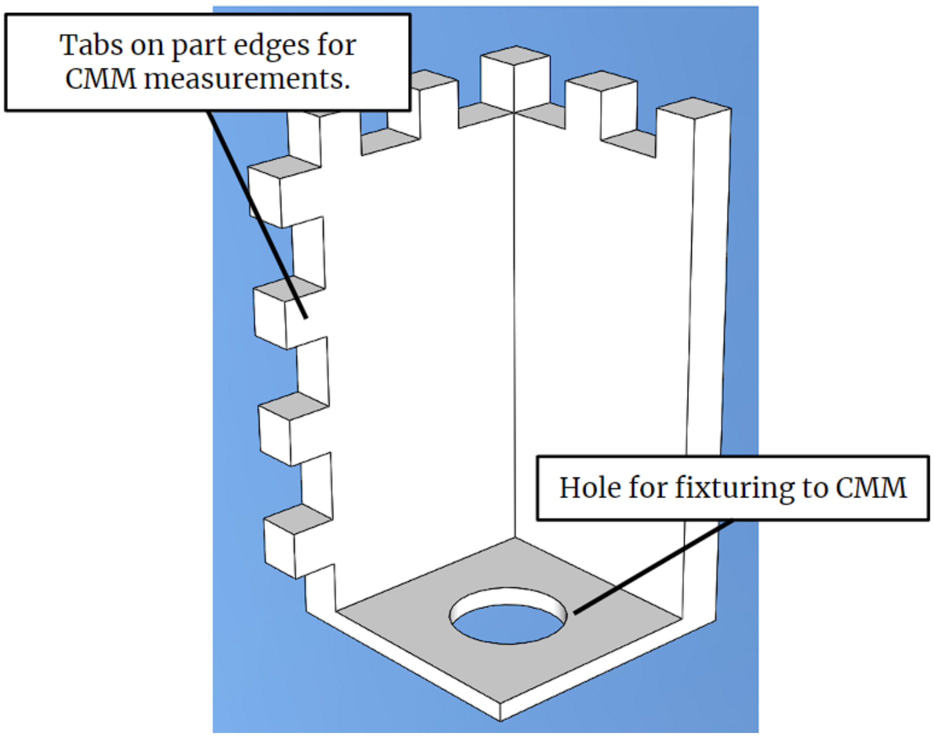

Figure 22: The small tabs on the outer edges allow the CMM to measure the linear accuracy of the part in all three axes across parts #1 and #2.

3.7 Minimum Resolvable Feature

Minimum feature size is qualitative data measured by observing each printed part for which features resolved and which did not. Similar to the study by Seepersad et al. [27], "pass/fail" criteria are applied to the features in parts #1 and #2 to evaluate the resolution of the PolyJet process, similar to the one shown in Figure 23.

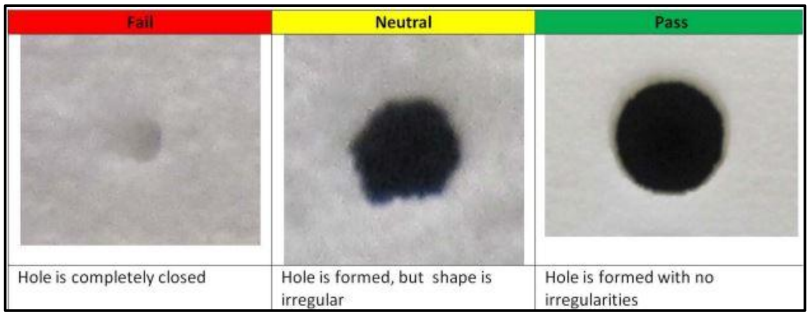

Figure 23: Pass/Fail criteria for resolution of holes built with polymer SLS; each level of resolution is designated with a color: green for a pass, red for a failure, and yellow for features that do not fall into either category.

Each geometric feature in each test part is evaluated for the minimum feature size and compiled into design guidelines for resolving multi-material and single-material features. Based on other metrology studies, we can expect to see the limits of PolyJet resolution within the specified size ranges for each feature. Table 4 highlights how the data for the minimum resolvable holes is compiled. The data is presented as a percentage to show how well a particular feature resolved across all test parts (e.g., 4mm circle that resolved in 3 out of 6 test parts would be 50%) to inform the designer how likely a feature is to resolve for a feature type, size, and orientation.

Table 4: Shows how minimum feature size data is compiled and categorized for circular features. A pass is marked by a green highlight, neutral with yellow, and a failure with red.

1-25%	FAIL										
25-75	NEUTRAL										
>75	PASS										
Multi-Material Circular Features											
Diameter (mm)	**4**	**3.5**	**3**	**2.5**	**2**	**1.5**	**1**	**0.8**	**0.6**	**0.4**	**0.2**
XY											
Z											
Single-Material Circular Features											
Diameter (mm)	**4**	**3.5**	**3**	**2.5**	**2**	**1.5**	**1**	**0.8**	**0.6**	**0.4**	**0.2**
XY											
Z											

Chapter 4: Results & Discussion

4.1 Minimum Feature Size Measurements

Microscope images of the parts were processed with ImageJ, an image-processing software. In ImageJ, test part images were converted into greyscale images and adjusted with image thresholding. Image thresholding works by choosing a pixel value cut-off, such that every pixel less than that value is considered white, and pixels greater than that value are considered black [28]. Thresholding helps identify how clearly defined the outline of the feature is relative to a "ground truth" of color intensity. The ground truth threshold was set at a value of 75. This threshold value was chosen since it captures the first peak on the intensity corresponding with the features. Figure 24 shows the thresholding tool in ImageJ and the pixel intensity spectrum.

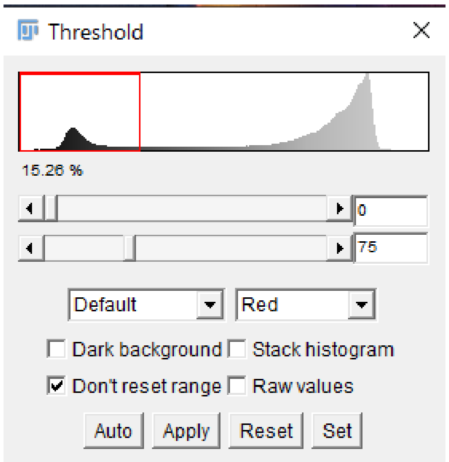

Figure 24: Pixel intensity values for an image of a geometric feature. A threshold value of 75 captures the intensity curve corresponding to the geometric feature's intensity.

With the threshold settings, criteria were formed for each geometric feature type. A passing feature is clear and well-defined by the threshold. A feature classified as neutral is still legible, but the edges are no longer clear and well-defined from the threshold. A feature is considered a failure if the threshold filter cannot outline the shape of the text. Figure 25 shows the criteria for multi-material text resolution based on a threshold of 75. (See Appendix I for the resolution criteria for all geometric features in parts #1 and #2.)

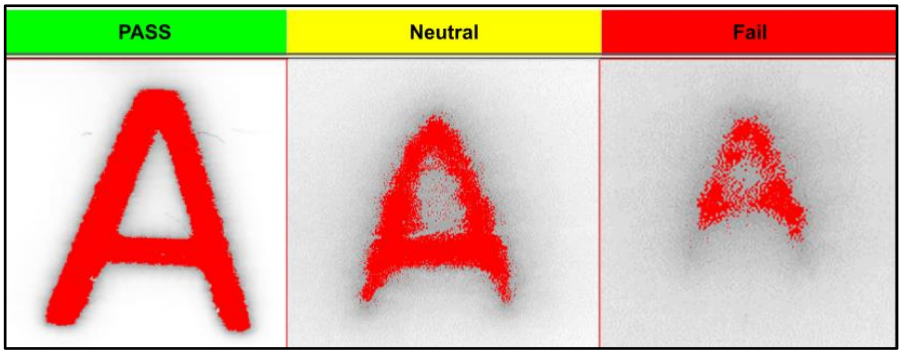

Figure 25: Multi-material text features were evaluated using the criteria above.

This thresholding technique was applied to all geometric features on parts #1 and #2. For part #2, the features are made with contrasting colors, so they are much easier to threshold for evaluating the minimum resolution. Part #1 was made from a single material and had voids instead of material in each geometric feature. To threshold single-material features, the microscope lighting is set low for the best contrast between the voids and surrounding material.

4.2 Minimum Feature Size Results & Discussion

The data for the minimum resolvable feature was determined based on the thresholding criteria for each feature type. If a feature is successfully resolved, a value of "2" is tabulated. If the feature falls under the "neutral" category, a value of "1" is tabulated. If a feature fails, a "0" is tabulated for that feature. The total across all test parts is divided by the maximum achievable "score" (# of test parts x 2). The instances of resolved features across the test parts are color-coded to highlight the percentage of resolved features. Tables 5 – 8 show the color charts reflecting the results for the minimum resolvable feature:

- RED (successfully resolves 0%-25% of the time): The feature failed to resolve across test parts consistently and is unlikely to resolve in other builds.
- YELLOW (resolves 25% - 75% of the time): The feature resolved across some test parts, which is not ideal for reliable design.
- GREEN (resolves > 75% of the time): Reliably resolved across most test parts and is ideal for design.

4.2.1 Circular features

Table 5: Color chart for circular features with various material (Single and Multi) and orientation (XY and Z) configurations.

Multi-Material Circular Features											
Diameter (mm)	4	3.5	3	2.5	2	1.5	1	0.8	0.6	0.4	0.2
XY	100.0	100.0	100.0	100.0	100.0	100.0	75.0	66.7	58.3	16.7	0.0
Z	100.0	100.0	100.0	100.0	100.0	91.7	66.7	50.0	33.3	0.0	0.0
Single-Material Circular Features											
Diameter (mm)	4	3.5	3	2.5	2	1.5	1	0.8	0.6	0.4	0.2
XY	100.0	100.0	100.0	91.7	83.3	58.3	50.0	41.7	0.0	0.0	0.0
Z	100.0	100.0	100.0	100.0	91.7	58.3	50.0	50.0	25.0	0.0	0.0

Multi-material circles built in the XY orientation resulted in the highest percentage of successful resolution across all test parts.

Explanation:

Circles built in the XY orientation are not impacted by the stair-stepping effect that typically affects inter-layer curved geometries. Nozzle and droplet size will likely directly impact features built in the XY orientation, making curved features like circles resolve more consistently. Overall, the best practice for reliably resolving circular features is to employ a multi-material feature in the XY orientation.

4.2.2 Text Features

Table 6: Color chart for text features with various material (Single and Multi) and orientation (XZ and Z) configurations.

Multi-Material Text											
Font Size	**18**	**16**	**14**	**12**	**10**	**9**	**8**	**7**	**6**	**5**	**4**	**3**
XY	100.0	100.0	100.0	100.0	91.7	83.3	66.7	50.0	16.7	8.3	0.0	0.0
Z	83.3	100.0	100.0	100.0	100.0	66.7	50.0	41.7	41.7	0.0	0.0	0.0
Single-Material Text												
Font Size	**18**	**16**	**14**	**12**	**10**	**9**	**8**	**7**	**6**	**5**	**4**	**3**
XY	100.0	91.7	83.3	50.0	41.7	33.3	0.0	0.0	0.0	0.0	0.0	0.0
Z	100.0	100.0	75.0	50.0	41.7	33.3	25.0	8.3	0.0	0.0	0.0	0.0

Text is primarily used in the context of multi-material printing. The data shows that text as a debossed feature in a single-material part does not consistently resolve. For the best results, multi-material text built in the XY orientation resulted in the highest percentage of successful resolution across all test parts.

Explanation:

The multi-material text was more consistently resolved due to the contrast between the two materials. Due to the lack of contrast between the text and surrounding part, single-material features did not consistently resolve via the thresholding criteria. When reading text, the contrast between the text and its medium makes the text legible regardless of the font size. Additionally, the XY orientation resulted in more successful text resolution due to the reduced material strands on the edges of the feature. Text built in the Z-orientation had large material strands that affected its appearance. A sudden discontinuity in the material jetting process likely causes the strands to appear in the text, as shown in Figure 26.

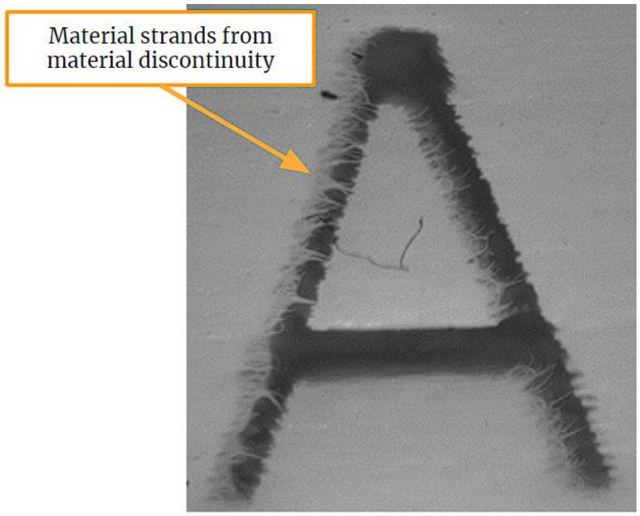

Figure 26: Material strands resulting from sudden discontinuity in jetting affect the resolution of the text.

4.2.3 Rectangular features

Table 7: Color chart for rectangular features with various material (Single and Multi) and orientation (XZ and Z) configurations.

Multi-Material Rectangular Features												
Dimensions (mm)	**6 x 3**	**5.4 x 2.7**	**4.8 x 2.4**	**4.2 x 2.1**	**3.6 x 1.8**	**3 x 1.5**	**2.4 x 1.2**	**1.8 x 0.9**	**1.2 x 0.6**	**0.6 x 0.3**	**0.4 x 0.2**	**0.2 x 0.1**
XY	100.0	100.0	100.0	100.0	100.0	100.0	58.3	58.3	50.0	8.3	0.0	0.0
Z	100.0	100.0	100.0	100.0	100.0	100.0	83.3	50.0	50.0	8.3	0.0	0.0
Single-Material Rectangular Features												
Dimensions (mm)	**6 x 3**	**5.4 x 2.7**	**4.8 x 2.4**	**4.2 x 2.1**	**3.6 x 1.8**	**3 x 1.5**	**2.4 x 1.2**	**1.8 x 0.9**	**1.2 x 0.6**	**0.6 x 0.3**	**0.4 x 0.2**	**0.2 x 0.1**
XY	100.0	100.0	91.7	100.0	100.0	75.0	66.7	50.0	50.0	25.0	0.0	0.0
Z	91.7	100.0	100.0	100.0	100.0	100.0	66.7	50.0	50.0	16.7	0.0	0.0

Explanation:

For rectangular features, feature resolution was relatively the same across the different material and orientation configurations. This shows that rectangular features are more predictable in resolution. In future studies, it may be useful to observe the resolution of rectangular features for other material configurations to determine if the resolution remains consistent.

4.2.4 Angled Faces

Table 8: Color chart for angular features with various material (Single and Multi) and orientation (XZ and Z) configurations.

Multi-Material Angles										
Angles	**90**	**81**	**72**	**63**	**54**	**45**	**36**	**27**	**18**	**9**
XY	100.0	100.0	100.0	100.0	100.0	100.0	75.0	58.3	41.7	0.0
Z	100.0	100.0	100.0	100.0	91.7	100.0	83.3	75.0	50.0	16.7
Single-Material Angles										
Angles	**4**	**3.5**	**3**	**2.5**	**2**	**1.5**	**1**	**0.8**	**0.6**	**0.4**
XY	100.0	91.7	100.0	100.0	100.0	83.3	66.7	50.0	16.7	0.0
Z	83.3	100.0	100.0	100.0	83.3	83.3	58.3	50.0	50.0	0.0

Explanation:

Multi-material features demonstrated slightly better resolution compared to single-material features in both orientations. Printing angles with the single-material configuration results in a small gap between the adjacent surfaces, likely fusing at the smaller angles because the material from the roller blade may fall into the gap and form agglomerates, making the multi-material configuration more suitable for resolving small angles.

4.2.5 Recommendation

Rather than highlighting a single dimension for each feature type, the percentage in the color charts allows a designer to make an informed decision about how reliably a feature resolves, even if it "neutrally" resolves. For example, if a part requires embedded text, the designer can determine whether to use a particular font size depending on the part application. If a part is produced in large quantities, only using font sizes that consistently resolve may be advantageous. A similar argument may be applied to feature dimensions.

4.3 Feature Accuracy Measurements

Since multi-material features cannot be measured with the CMM, a microscope was used to measure the geometric accuracy of the circular and rectangular features. Microscope images of the test parts are taken with an AmScope-SM-1TNZ-144A-10M Stereomicroscope and measured with the microscope software. The microscope is calibrated with a 1mm standard to relate pixels to a physical distance, and then the software is used to measure critical feature dimensions. Due to the geometry of the test parts, they are fixtured onto a small block that ensures each part is the same distance from the microscope. Figure 27 shows the microscope setup for measuring features and imaging parts.

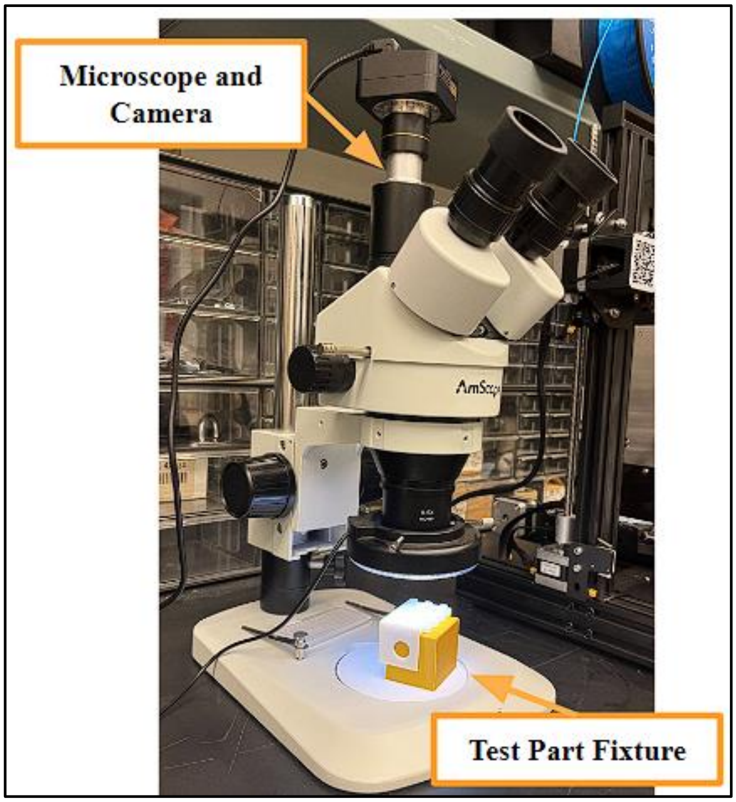

Figure 27: AM Stereomicroscope with a microscope camera is used for imaging and measuring test parts. All test parts are fixtured onto a small block for consistent imaging.

These measurements were made based on the best visual approximation of feature outlines and are limited by the operator's ability to measure each feature consistently and accurately. However, to compare the performance of the different feature configurations, they needed to be measured with the same tools and methods. Each feature was measured twice in different sections to mitigate user bias. Figure 28 shows how measurements were taken for each rectangular and circular feature.

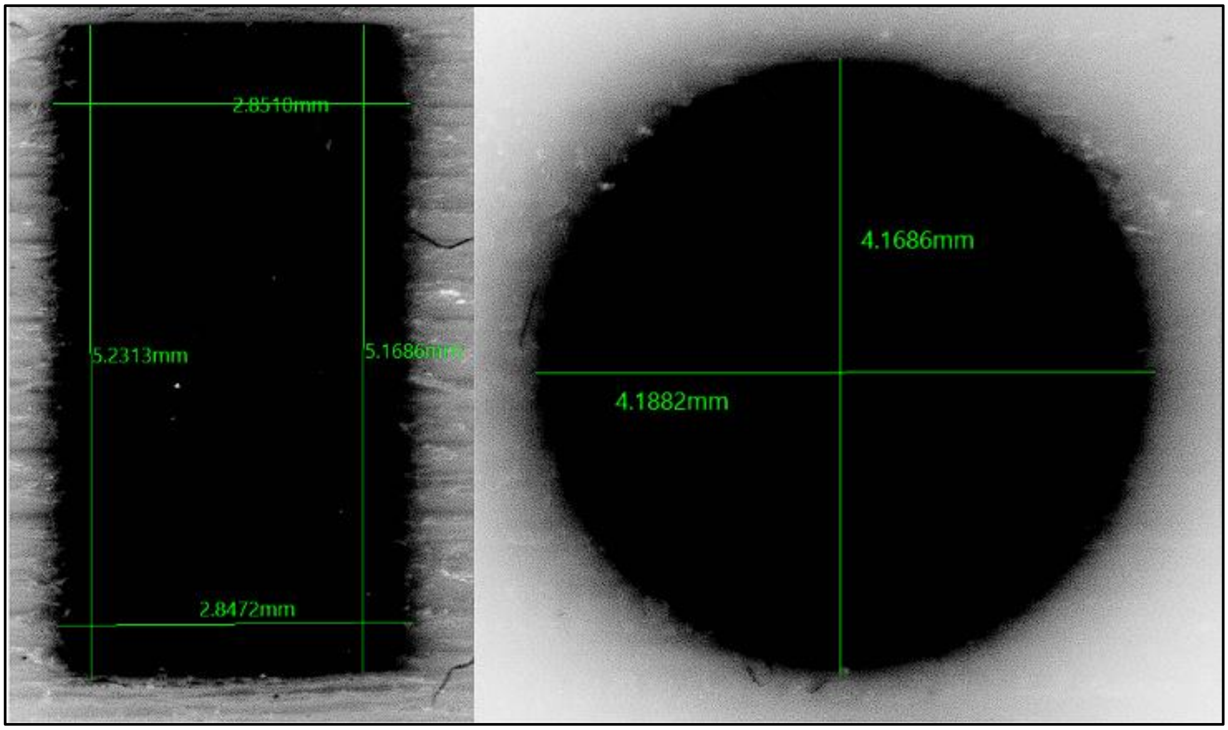

Figure 28: Microscope images of rectangular and circular features are measured with a digital tool. Two measurements are taken for the diameter of circular features and 2 measurements of length and width for rectangular features.

4.4 Feature Accuracy Results & Discussion

After measurement data for each geometric feature was collected from parts #1 and #2, it was categorized to form four principal observations:

1.) How the material configuration (multi vs. single) impacts the geometric accuracy of circular features built in the Z orientation.

2.) How the material configuration (multi vs. single) impacts the geometric accuracy of circular features built in the XY orientation.

3.) How the material configuration (multi vs. single) impacts the geometric accuracy of rectangular features built in the Z orientation.

4.) How the material configuration (multi vs. single) impacts the geometric accuracy of rectangular features built in the XY orientation.

4.4.1 Measurement Analysis

The data for each observation was sorted in Excel, the average measurement for each feature was taken, and the standard deviation of the measurements was used to compute the Standard Deviation Index (SDI). The SDI, also known as a Z-score, measures how many standard deviations a measurement is from a target value. SDI is typically used when comparing new measurements to historical data for a measurement apparatus. SDI determines how many standard deviations the average measured values are from the nominal dimensions. The following formula is used to calculate the SDI present in each dimension:

$$SDI = (Nominal\ Value - Measured\ Mean)/(Measured\ Standard\ Deviation)$$

The absolute SDI values across all measurements are then averaged to determine how many standard deviations, on average, measurements deviate from the nominal dimensions. The tabulated data and SDI values are shown in Tables 13-15 in Appendix III. On average, all measured data lie within less than 1 standard deviation from the nominal values. Conversely, this indicates that the measured data is within an acceptable range with minimal bias. It is worth noting that data was limited for small features that did not resolve and could not be measured. Figures 29 – 32 visually demonstrate how the average measured values for each feature compare to the nominal dimensions. For the plots, data is plotted against the nominal dimensions in both x and y. For circular features, the y-axis represents the nominal values, while the x-axis denotes which circular feature is being compared (e.g., diameter of 4 mm is the largest, therefore the 11th feature). For rectangular features, the x and y axes correspond to nominal length and width, respectfully.

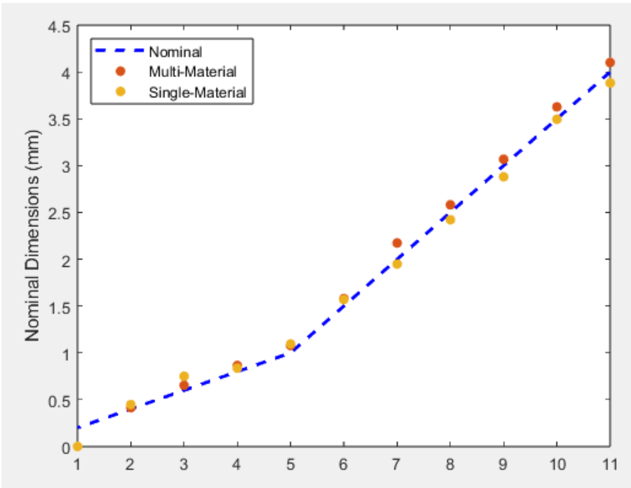

Figure 29: Average geometric accuracy of multi- and single-material circular features built in the XY orientation. Avg Multi SDI: 0.9264, Avg Single SDI: 0.7305

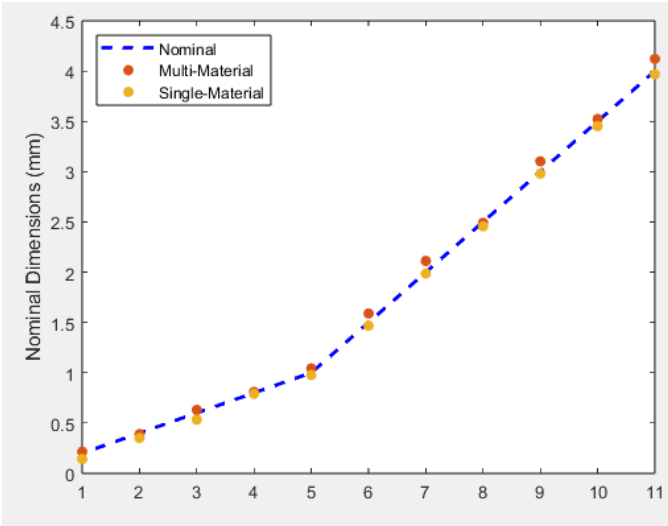

Figure 30: Average geometric accuracy of multi- and single-material circular features built in the ZY orientation. Avg Multi SDI: 0.3595, Avg Single SDI: 0.4204

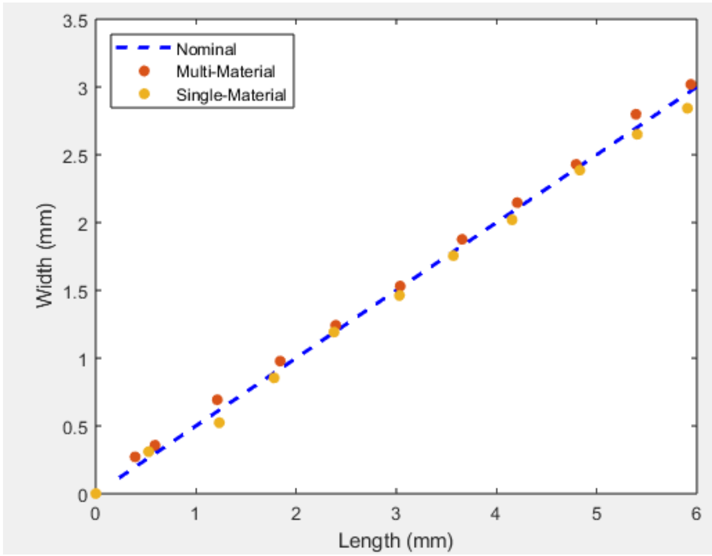

Figure 31: Average geometric accuracy of multi- and single-material rectangular features built in the XY orientation.

Avg Multi SDI (L, W): (0.3079, 0.8330), Avg Single SDI (L, W): (0.5426, 0.6929)

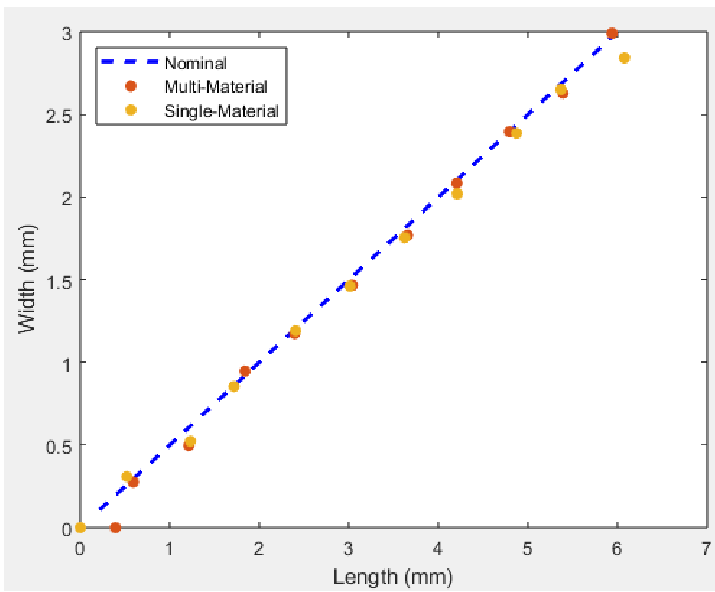

Figure 32: Average geometric accuracy of multi- and single-material rectangular features built in the Z orientation.

Avg Multi SDI (L, W): (0.3634, 0.7939), Avg Single SDI (L, W): (0.3837, 0.5395)

4.4.2 Explanation

The average SDI values for the measurement data were low across the geometric features meaning that, on average, all as-built dimensions were quite accurate relative to nominal dimensions for their respective categories. The low SDI values across all features indicates that the accuracy was consistently good for all measurements.

In addition to the SDI, the percentage error for the average measurement values compared to the nominal values was computed (Shown in Tables 13-16 in Appendix III). Note that cells denoted with an "NA" were features that failed to resolve and could not be measured.

The deviation from nominal values increased significantly for smaller features, likely due to the increased difficulty in the measurement process. Additionally, the manufacturer specifies much higher accuracy in the Z-direction compared to the X and Y directions. This trend was not observed in this study. It is possible that the measurement methods may not be accurate enough to capture significant differences in the geometric accuracy across the various feature categories. The measurement of the geometric features was limited to optical measurements, making the microscope camera's resolution, coupled with the material strand effect, the limiting factors in the accuracy measurements.

4.5 Overall Geometric Accuracy

In addition to the optical measurements, all 12 parts were evaluated for geometric accuracy in the X, Y, and Z build axes with a *Zeiss Spectrum Coordinate Measuring Machine*. Parts #1 and #2 have three sets of tabs on their outer edges, each printed along one of the build axes for measuring the general accuracy of the part in all three directions. Two linear measurements were taken in each direction relative to an outer datum plane, one measurement at

12.5 mm and another at 25 mm from the datum. The datum plane for each axis corresponds to the first surface from which the measurements are taken. Figure 33 shows the datum planes and corresponding tab measurements.

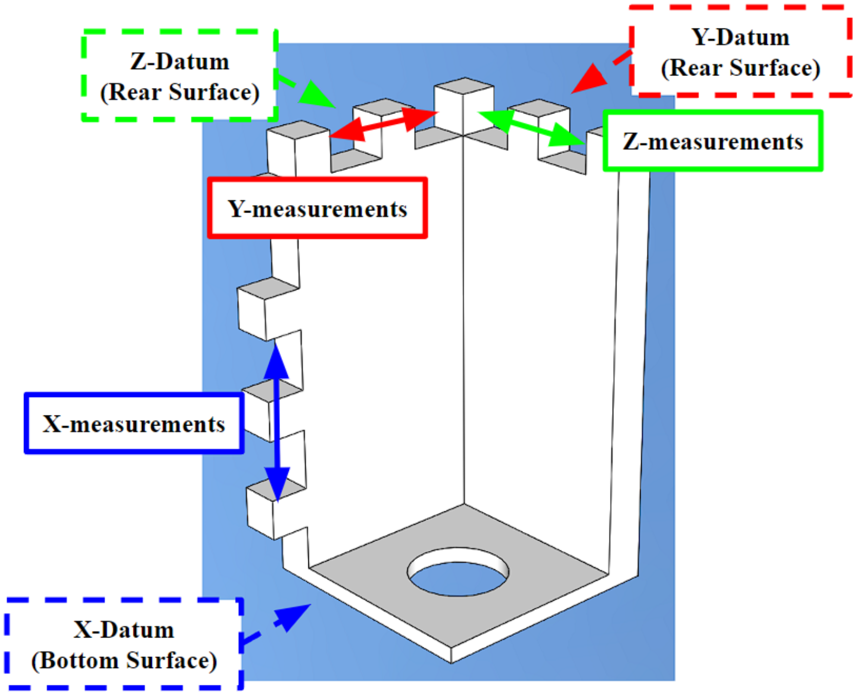

Figure 33 :Measurements for each axis are taken from the outlined datum planes. The features are measured with a CMM to determine the linear accuracy in each axis.

4.6 Overall Geometric Accuracy Results & Discussion

Since test parts #1 and #2 have the same geometry, the measurement tabs are unaffected by the material configuration. All 12 parts were measured with the same CMM stylus (3 mm diameter) and fixture shown in Figure 34. Once fixtured onto the CMM, each part was measured and the CMM output a file with the programmed measurements. Figures 35 and 36 show the measurement data from the CMM plotted to show how the measured data for each part deviated from the nominal values.

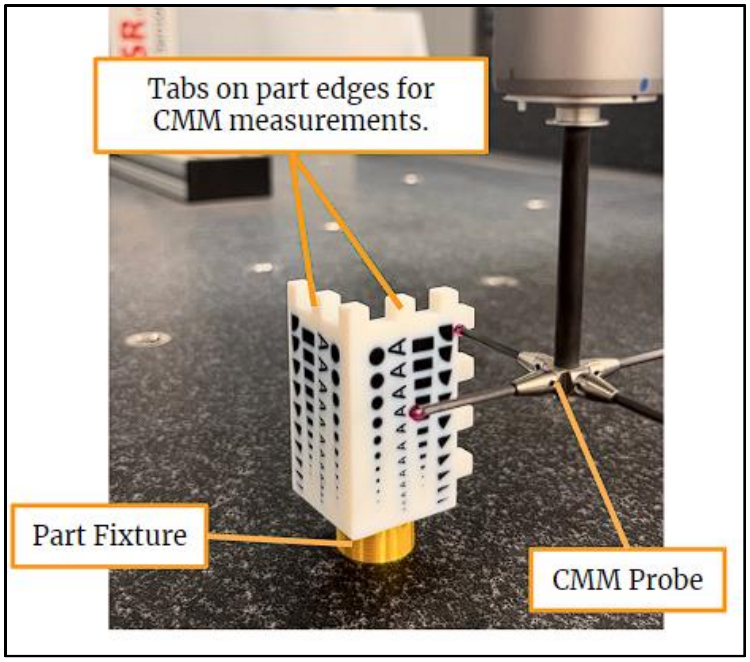

Figure 34: Measurement configuration of linear accuracy in test parts on the CMM.

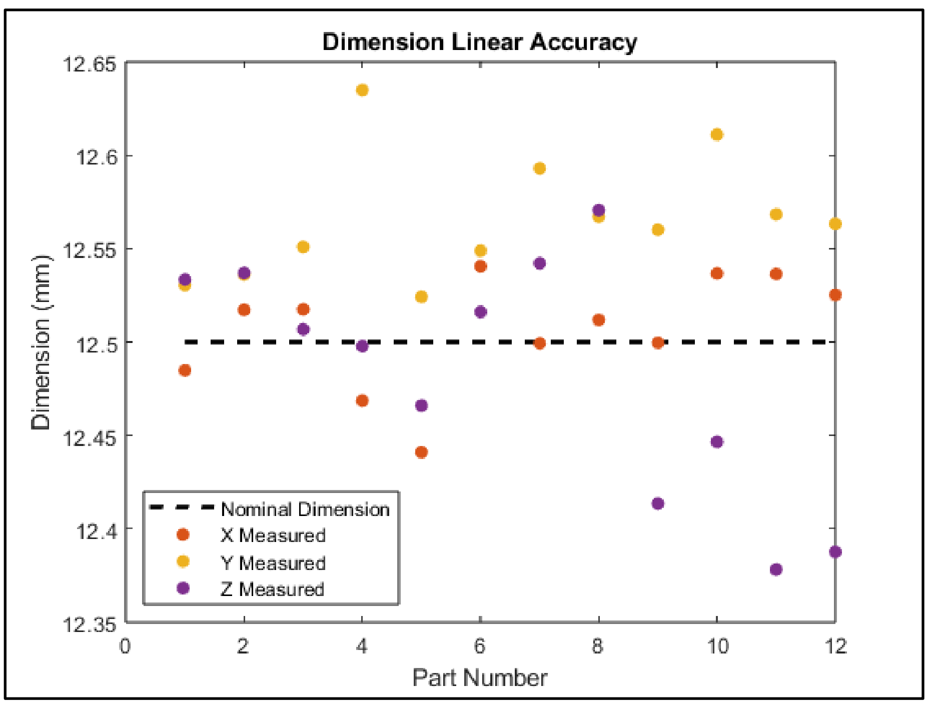

Figure 35: The linear accuracy measurements for each part are shown for the expected value of 12.5 mm in each axis.

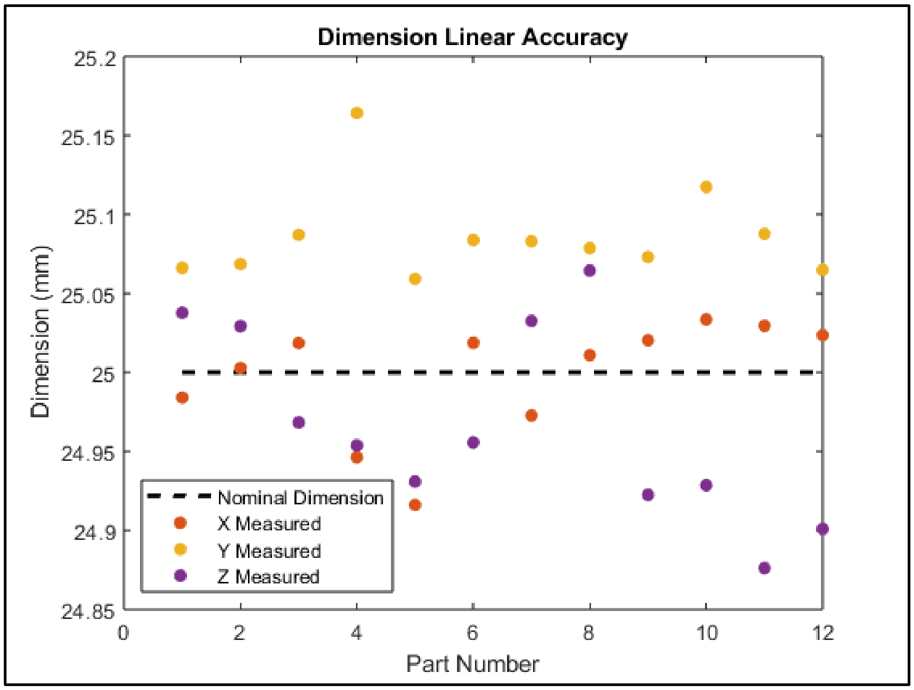

Figure 36: The linear accuracy measurements for each part are shown for the expected value of 25 mm on each axis.

4.6.1 Explanation

The accuracy of the parts in all three axes demonstrated an error of less than 1%. All measurements in the y-axis were slightly larger than the nominal value and demonstrated the highest average deviation from the nominal values across both measurements. The measurements in the X direction exhibited the best overall accuracy with the smallest average deviation, as shown in Table 9. The CMM has a theoretical tolerance of ± 3 µm, however, the error from the CMM for the part measurements was reported to be ± 100 µm. The larger tolerance could be partially due to the size of the CMM stylus used to measure the parts which had a diameter of 3 mm. For future studies, a CMM-specific test part should be designed to accommodate a smaller stylus.

Table 9: Average deviation of linear measurements from the nominal value in each axis on the test parts.

Axis	Average Deviation
X-Direction	+2.3 µm
Y-Direction	+75.9 µm
Z-Direction	-25.1 µm

4.7 Survivability Measurements

As previously mentioned, parts printed with the PolyJet process typically have support material that needs to be removed in post-processing. Parts are typically cleaned with a high-pressure jet stream that can be destructive for small features. However, additional cleaning tools and different water stream nozzles can help improve the survivability of post-processed features. To identify better alternatives to the traditional cleaning method, two techniques were used to evaluate how different post-processes impact the survivability of small geometric features printed with PolyJet:

- **Technique #1** – Parts are cleaned with the jet stream for two minutes.
- **Technique #2** – Parts are cleaned with a flat tip stream for two minutes.

If a feature survived, a 1 was placed on the chart, versus a 0 if the feature did not survive. Data for the minimum survivable feature was color coded with criteria similar to the minimum resolvable feature data:

- RED (resolves 0%-25% of the time): The feature does not consistently survive post-processing and is likely to fail.
- YELLOW (resolves 25% - 75% of the time): The feature sometimes survives across test parts but is not ideal for a reliable design.

- GREEN (resolves > 75% of the time): The feature consistently survives post-processing across most test parts and is ideal for reliable resolution.

4.8 Survivability Results & Discussion

Test parts were removed from the print bed, and the bulk material was removed from the outer surfaces. Bulk material includes large masses on the part's outer surfaces, typically removed with mechanical tools to make the water jet cleaning process more effective. Once the bulk of support material was removed, the parts were cleaned in the support removal station shown in Figure 37.

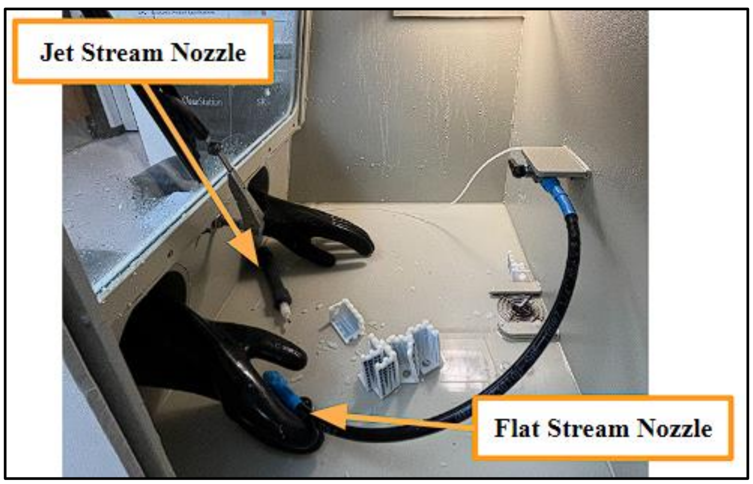

Figure 37: The water jet cleaning station for post-processing PolyJet parts is a small glovebox with hoses for different nozzle attachments.

4.8.1 Technique #1

Table 10:Survivability data for parts cleaned with technique #1: jet stream spray for 2 minutes

Jet Stream								
Fixed								
	0.25	0.5	0.75	1.0	1.25	1.5	1.75	2.0
Rectangular Z	0	0	0	0	0	100	100	100
Rectangular Y	0	0	60	100	100	100	100	100
Circular Z	0	0	0	0	0	80	100	100
Circular Y	0	0	60	100	100	100	100	100
Cantilever								
	0.25	0.5	0.75	1.0	1.25	1.5	1.75	2.0
Rectangular Z	0	0	0	0	0	0	40	40
Rectangular Y	0	0	0	0	40	80	100	100
Circular Z	0	0	0	0	0	0	20	20
Circular Y	0	20	0	0	20	60	100	100

Features cleaned with technique #1 exhibited poor survivability for circular columns built in the Z-direction and the best resolution for rectangular features built in the Y-direction. Figure 38 shows images of the part after cleaning with technique #1.

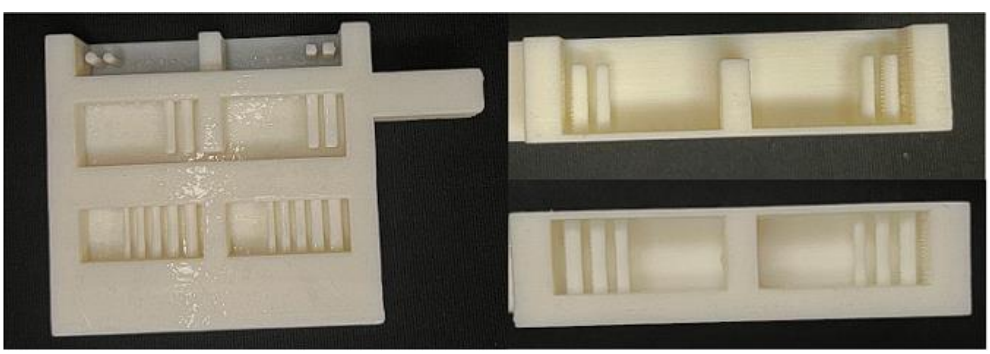

Figure 38: The survivability test part cleaned with technique #1 shows poor survivability for most column configurations.

4.8.2 Technique #2

Table 11: Survivability data for parts cleaned with technique #2: flat nozzle spray for two minutes.

Flat Spray								
Fixed								
	0.25	0.5	0.75	1.0	1.25	1.5	1.75	2.0
Rectangular Z	0	0	0	20	100	100	100	100
Rectangular Y	60	100	100	100	100	100	100	100
Circular Z	0	0	0	0	100	100	100	100
Circular Y	40	100	100	100	100	100	100	100
Cantilever								
	0.25	0.5	0.75	1.0	1.25	1.5	1.75	2.0
Rectangular Z	0	0	0	20	100	100	100	100
Rectangular Y	20	20	80	100	100	100	100	100
Circular Z	0	0	0	0	80	100	100	100
Circular Y	20	20	40	80	100	100	100	100

Consistent with the jet stream data, features built in the Y-direction exhibited the highest survivability across test parts due to the intralayer surfaces, which resist the force from the pressurized stream. Figure 39 shows images of the part after cleaning with technique #2.

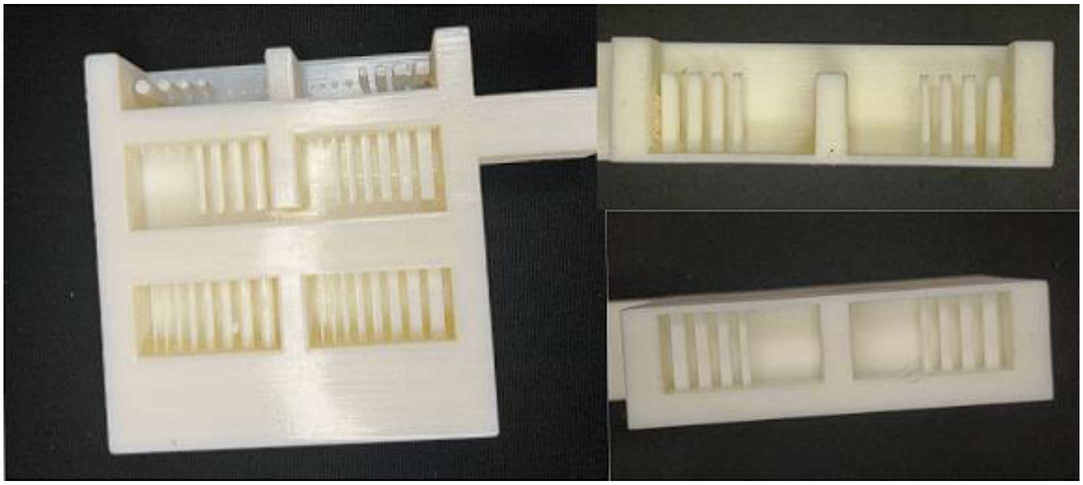

Figure 39: Parts cleaned with technique #2 exhibit good survivability due to the gentler cleaning methods. However, there is still some remaining support material.

Images of the test part show that immediately after cleaning with the flat tip spray, there are still small amounts of support material left on some of the columns. The parts were soaked in a NaOH solution to remove any remaining support. The solution did not impact feature survivability.

4.8.3 Analysis

4.8.3-C Cross-sectional Shape

All features were fabricated with the same dimension in the width of the part (diameter for circular and width for rectangular). However, since the shapes are different, the cross-sectional areas of the features make them hard to compare. The results still serve as a guide for designers to resolve circular or rectangular features within the tested dimension ranges. In future experiments, the test part can be modified to compare the cross-sectional shapes and their impact on survivability.

4.8.3-D Feature Orientation

How the material layers form geometry can explain the disparity in the survivability for build orientation. Features built in the Z-direction are interlayer, meaning the layers stack along the height of the column, making it easier for the jet stream to split the geometry between layers. Figure 40 demonstrates how the water jet interacts with features built both interlayer and intralayer.

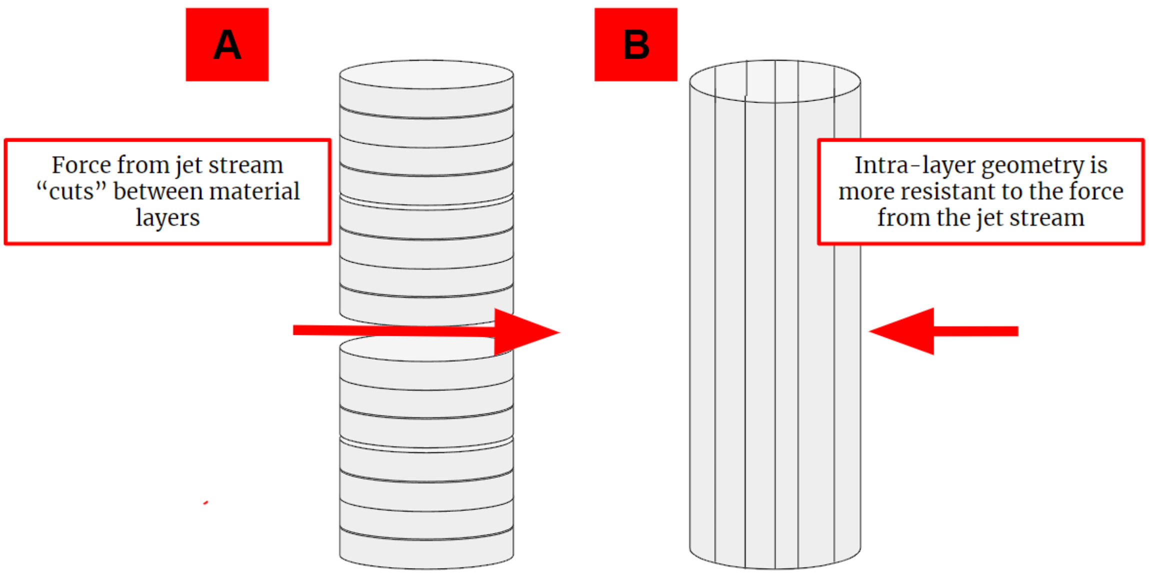

Figure 40: How water stream interacts with interlayer features (A) vs. intralayer features (B).

If the standard cleaning jet stream is the only available cleaning method, it is recommended to avoid thin interlayer features overall. It is important to note that the feature size is the main contributor to the increased survivability of rigid features built in the Z-direction, meaning that the larger a feature is, the more likely it is to survive. The data shows that it is best to clean small features with less abrasive methods, such as the flat stream nozzle, and supplement by soaking parts in a NaOH solution.

Chapter 5: Closure

5.1 Summary

Chapter 1 establishes the need to conduct a metrology study for the PolyJet process to create a design for additive manufacturing (DfAM) framework that enables standard product definition practices for PolyJet. Understanding the bounds of the capability of an AM process helps designers make informed decisions when defining a product. PolyJet, which has various materials and unique capabilities, would benefit significantly from product definition practices like Model-Based Definition (MBD), which can capture the product and manufacturing information associated with the PolyJet process.

Chapter 2 summarizes prior metrology studies performed on the PolyJet process and their use of benchmark test parts. Meisel et al. [8] conducted a study using several benchmark parts to characterize the capability of PolyJet to resolve unsupported overhangs, debossed holes/slots, feature survivability, and embossed holes/slots. However, this study did not explore multi-material capabilities or the impact of build orientation on geometric performance. Tee et al. [19] explored using multi-material feature metrology for PolyJet but did not expand on the effects of build orientation on the geometric features. As part of characterizing PolyJet, there is also a need to characterize different machines. Many studies identified in the literature did not perform metrology studies on the machine available for this work, the Stratasys J750. The review of prior studies identified several gaps in knowledge to be addressed with a metrology study and a new benchmark test part.

The details of the metrology study and test parts used in the proposed study are outlined in Chapter 3. Three test parts were designed for the metrology study. Test part #1 evaluates

PolyJet's capability to resolve various single-material debossed features. Test part #2 examines PolyJet's ability to resolve various multi-material geometric features compared to single-material features. Test part # 3 determines how build orientation, fixture connectivity, and different support removal techniques affect the survivability of small column-like features. A total of 22 parts were built: six for test part #1, six for test part #2, and 10 for test part #3. A digital microscope was used to measure the features on parts #1 and #2 and determine the geometric fidelity of single-material and multi-material features built in the XY and Z orientations. An image threshold was applied to images of parts #1 and #2 to determine the minimum resolvable feature based on pass/fail criteria. Test parts #1 and #2 included small tabs on the outer edges that were measured for overall linear accuracy in each build axis using a Coordinate Measurement Machine (CMM). For part #3, half of the parts were post-processed with the traditional water jet stream and the other half with a flat tip stream supplemented by a 60-minute soak in an alkaline solution. All the parts were then visually inspected to collect data for each feature on the part.

Chapter 4 presents the results of the metrology study and design guidelines for each of the explored design features. Results for minimum resolvable features are presented on color-coded charts that highlight the percentage of resolved features for each category. The color-coded charts serve as a visual indication of the reliability of a feature to resolve during printing. The results show that the contrast of the multi-material features make them more likely to resolve than single-material ones, especially for text features. The results of geometric accuracy are separated into two sections: 1) Geometric accuracy of geometric features measured with digital microscope images, 2) Geometric accuracy of parts in all three build axes measured with a CMM. The results for both accuracy experiments are presented with plots showing the average deviation of the measured values compared to nominal dimensions. The results for the accuracy of parts in the various dimensions are shown to be inconsistent with the accuracy specifications from the machine manufacturer. Features built in the Z orientation are expected to demonstrate the highest geometric fidelity. However, features built in the XY orientation demonstrate better geometric accuracy in general, with the X direction exhibiting the best linear accuracy. Similar to the minimum resolvable feature, results for survivability are also presented with color-coded charts to demonstrate the number of features that survive post-processing for two different cleaning techniques. The results show that when resolving small column-like features, the build orientation affects survivability because of how the force from the water stream interacts with the build layers. Features built with an intra-layer orientation exhibited higher levels of survivability. Additionally, using less abrasive cleaning techniques such as a flat-tip stream to remove the bulk of supports and soaking NaOH solution to dissolve remaining supports drastically improves the survivability of small geometric features.

5.2 Future work

The results gathered from this metrology study provide guidelines for designers to leverage for navigating the expansive design space afforded by PolyJet. However, the wide range of design capabilities associated with PolyJet manufacturing underlines the need to expand the characterization of additional machines, materials, and geometric features. There is an opportunity to create a repository for presenting results from additional PolyJet metrology studies and make them publicly available for other researchers to review or expand upon.

The results from the geometric accuracy study highlight a need to use more robust metrology tools, such as optical profilometry or X-ray computed tomography. Moreover, the number of parts used in the study could be increased to improve the statistical significance of the results and present other phenomena associated with resolving geometric features, such as the material strand effect present in this study.

Additionally, one of the main goals of this study is to contribute to the landscape of AM standardization and the widespread adoption of MBD for AM—further work on outlining a comprehensive product definition schema for products made with the PolyJet process is needed to realize the benefits of MBD. A future study could present a template for an MBD package that includes PolyJet design guidelines for researchers to use when creating new designs to print with PolyJet.

Appendix I Minimum feature size criteria

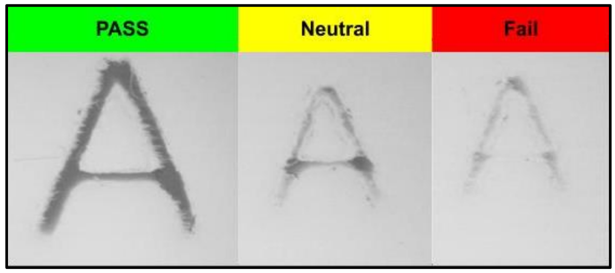

Figure 41: Single-material text minimum resolution criteria from microscope images.

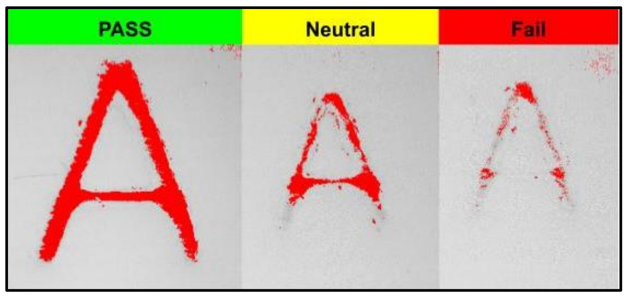

Figure 42: Single-material text minimum resolution criteria from thresholded images.

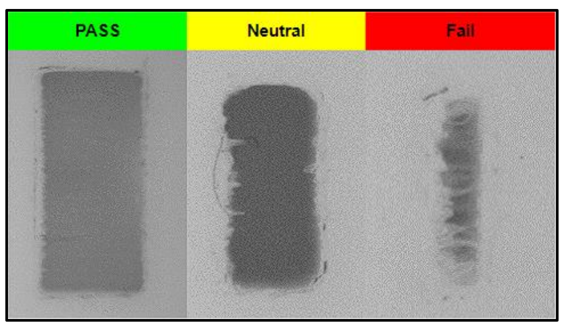

Figure 43: Single-material rectangular feature minimum resolution criteria from microscope images.

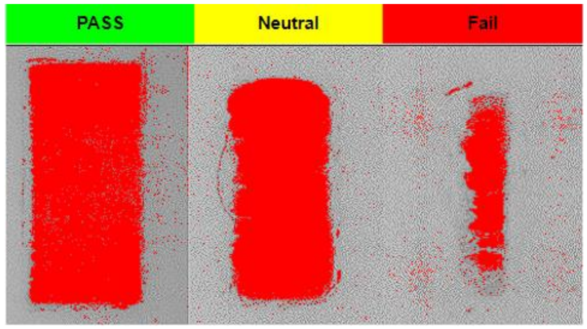

Figure 44: Single-material rectangular feature minimum resolution criteria from thresholded images.

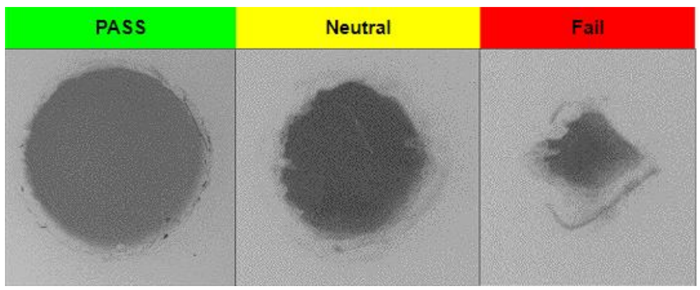

Figure 45: Single-material circular feature minimum resolution criteria from microscope images.

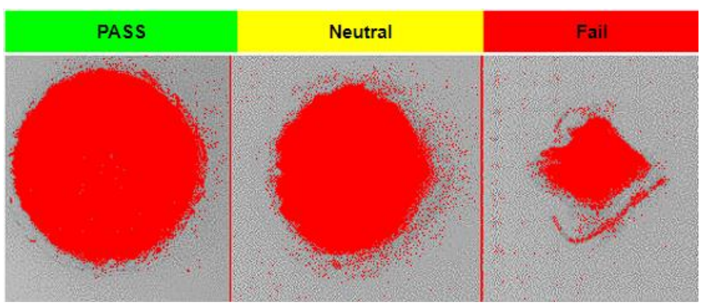

Figure 46: Single-material circular feature minimum resolution criteria from thresholded images.

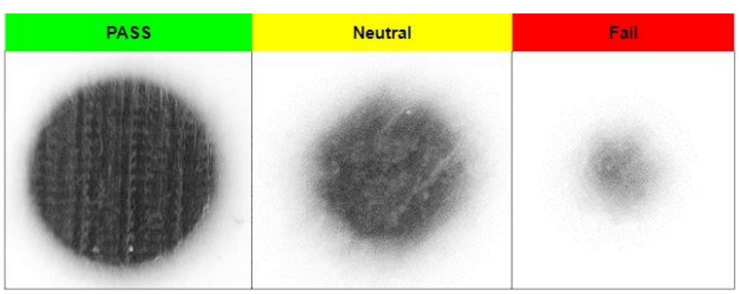

Figure 47: Multi-material circular feature minimum resolution criteria from microscope images.

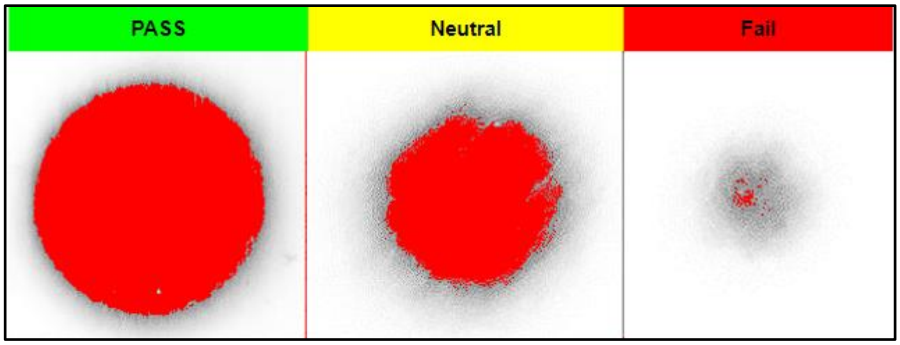

Figure 48: Multi-material circular feature minimum resolution criteria from thresholded images.

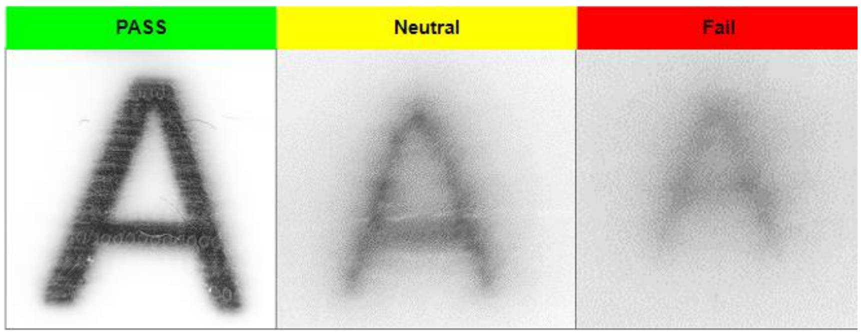

Figure 49: Multi-material text minimum resolution criteria from microscope images.

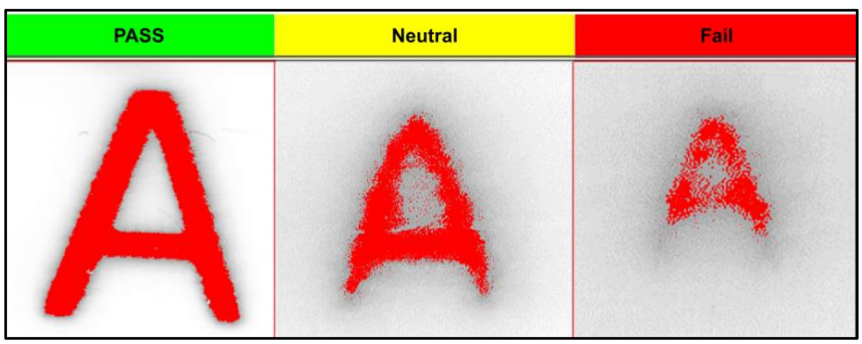

Figure 50: Multi-material text minimum resolution criteria from thresholded images.

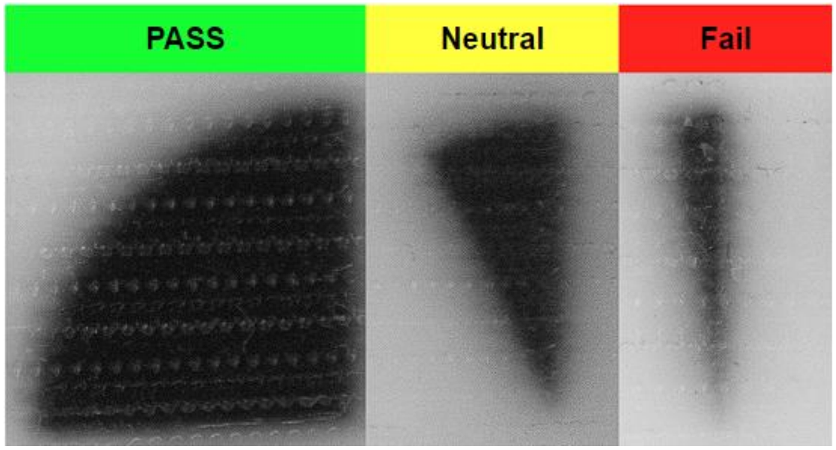

Figure 51: Multi-material text minimum resolution criteria.

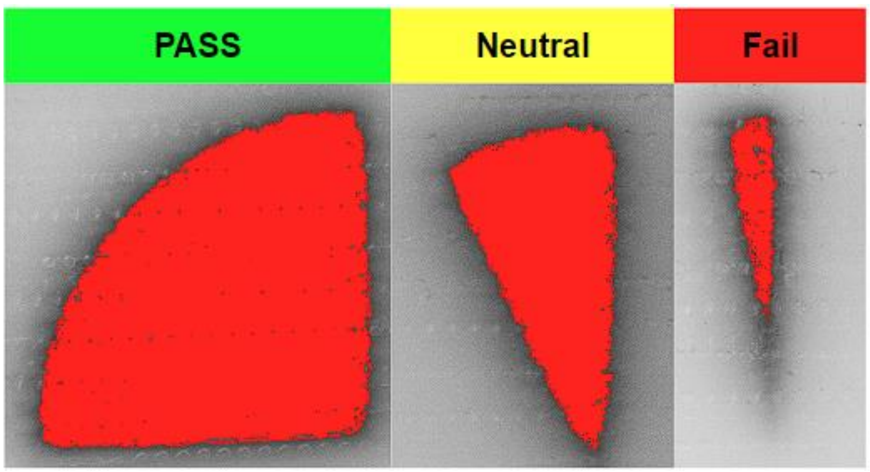

Figure 52: Multi-material text minimum resolution criteria-Thresholded.

Appendix II: CMM Accuracy

Table 12: Linear accuracy measurements for test parts #1 and #2 from CMM. It is important to note that the XYZ header is based on the CMM axes and not the build axes of the part.

Linear Accuracy							
PART #	**X1**	**X2**	**Y1**	**Y2**	**Z1**	**Z2**	**Z3**
P1	12.5334	25.0378	12.5304	25.0662	12.4848	24.9840	37.4852
P2	12.5370	25.0293	12.5361	25.0686	12.5172	25.0028	37.5144
P3	12.5068	24.9683	12.5509	25.0871	12.5175	25.0186	37.5479
P4	12.4978	24.9538	12.6348	25.1642	12.4686	24.9462	37.4640
P5	12.4660	24.9309	12.5242	25.0592	12.4410	24.9161	37.4199
P6	12.5161	24.9556	12.5488	25.0838	12.5405	25.0187	37.5596
P7	12.5421	25.0326	12.5929	25.0830	12.4993	24.9727	37.4891
P8	12.5706	25.0645	12.5671	25.0787	12.5118	25.0109	37.5196
P9	12.4135	24.9225	12.5601	25.0730	12.4996	25.0203	37.5049
P10	12.4466	24.9286	12.6110	25.1174	12.5367	25.0336	37.5382
P11	12.3783	24.8761	12.5683	25.0877	12.5364	25.0295	37.5403
P12	12.3877	24.9009	12.5632	25.0649	12.5252	25.0236	37.5120
AVG Dimension	12.4843	24.9693	12.5606	25.0795	12.5060	24.9982	37.5073
AVG Deviation	0.0513	0.0606	0.0657	0.0862	0.0243	0.0282	0.0316
err %	**0.4107**	**0.2425**	**0.5252**	**0.3446**	**0.1947**	**0.1130**	**0.2525**

Appendix III: Geometric Feature Accuracy

Table 13: Average measurements for circular features built in the XY orientation for both material configurations.

XY				
Diameter (mm)				
Nominal	**Average (Multi-material)**	**Average (Single-material)**	**SD Index Multi**	**SD Index Single**
4	4.1010	3.8824	1.2157	-0.6990
3.5	3.6274	3.4945	0.9408	-0.0781
3	3.0675	2.8805	0.8835	-0.7007
2.5	2.5809	2.4219	0.9778	-1.3197
2	2.1737	1.9483	1.1315	-0.7113
1.5	1.5800	1.5697	0.8604	0.3871
1	1.0775	1.0948	1.3277	0.4257
0.8	0.8658	0.8374	0.8052	0.3617
0.6	0.6532	0.7504	0.7316	0.8209
0.4	0.4140	0.4471	0.3893	1.8003
0.2	#DIV/0!	NA	#DIV/0!	NA
		Average Absolute SDI	**0.9264**	**0.7305**

Table 14: Average measurements for circular features built in the Z orientation for both material configurations.

ZY				
Diameter (mm)				
Nominal	**Average (Multi-material)**	**Average (Single-material)**	**SD Index Multi**	**SD Index Single**
4	4.1202	3.9677	0.4843	-0.2278
3.5	3.5235	3.4516	0.2176	-0.3504
3	3.1020	2.9799	0.5930	-0.1653

2.5	2.4913	2.4563	-0.0924	-0.4714
2	2.1114	1.9866	0.5287	-0.1554
1.5	1.5890	1.4678	0.6417	-0.3470
1	1.0432	0.9774	0.4482	-0.3169
0.8	0.8095	0.7900	0.1280	-0.3819
0.6	0.6297	0.5334	0.3082	-0.7152
0.4	0.3909	0.3512	-0.1526	-1.0731
0.2	0.2153	0.1422	#DIV/0!	NA
		Average Absolute SDI	**0.3595**	**0.4204**

Table 15: Average measurements for rectangular features built in the XY orientation for both material configurations.

XY					
Multi-Material					
Nominal Length (mm)	**Measured Length (mm)**	**Nominal Width (mm)**	**Measured Width (mm)**	**SD Index Length**	**SD Index Width**
6	5.9395	**3**	3.0181	-0.4626	0.1892
5.4	5.3912	**2.7**	2.7980	-0.0667	0.7387
4.8	4.7945	**2.4**	2.4283	-0.0894	0.5602
4.2	4.2066	**2.1**	2.1461	0.0513	0.6019
3.6	3.6559	**1.8**	1.8758	0.7343	0.7228
3	3.0375	**1.5**	1.5306	0.5901	0.7220
2.4	2.3948	**1.2**	1.2414	-0.0973	0.7001
1.8	1.8405	**0.9**	0.9772	0.5027	2.0600
1.2	1.2128	**0.6**	0.6924	0.3470	1.2472
0.6	0.5909	**0.3**	0.3569	-0.1373	0.7878
0.4	0.3922	**0.2**	0.2708	#DIV/0!	#DIV/0!
0.2	#DIV/0!	**0.1**	#DIV/0!	#DIV/0!	#DIV/0!
			Average Absolute SDI	**0.3079**	**0.8330**

XY					
Single-Material					
Nominal Length (mm)	**Measured Length (mm)**	**Nominal Width (mm)**	**Measured Width (mm)**	**SD Index Length**	**SD Index Width**
6	5.9051	**3**	2.8425	-1.0720	-1.4564
5.4	5.4037	**2.7**	2.6504	0.0489	-0.6682
4.8	4.8308	**2.4**	2.3860	0.1809	-0.1114
4.2	4.1545	**2.1**	2.0200	-0.4054	-0.8689
3.6	3.5691	**1.8**	1.7549	-0.6574	-1.2317
3	3.0309	**1.5**	1.4613	0.4229	-0.3968
2.4	2.3775	**1.2**	1.1911	-0.3277	-0.1018
1.8	1.7795	**0.9**	0.8538	-0.3082	-0.6509
1.2	1.2327	**0.6**	0.5230	1.3623	-0.8478
0.6	0.5275	**0.3**	0.3091	-0.6400	0.5953
0.4	#DIV/0!	**0.2**	#DIV/0!	#DIV/0!	#DIV/0!
0.2	#DIV/0!	**0.1**	#DIV/0!	#DIV/0!	#DIV/0!
			Average Absolute SDI	**0.5426**	**0.6929**

Table 16: Average measurements for rectangular features built in the Z orientation for both material configurations.

ZY					
Multi-Material					
Nominal Length (mm)	**Measured Length (mm)**	**Nominal Width (mm)**	**Measured Width (mm)**	**SD Index Length**	**SD Index Width**
6	5.9990	**3**	3.2217	-0.0126	1.1116
5.4	5.3578	**2.7**	2.7356	-0.5039	0.2776
4.8	4.7714	**2.4**	2.5340	-0.3151	0.8567
4.2	4.2085	**2.1**	2.2631	0.0675	1.0880
3.6	3.6189	**1.8**	1.8542	0.1728	0.8143
3	3.0390	**1.5**	1.5730	0.2936	0.7038
2.4	2.3925	**1.2**	1.2459	-0.0640	0.8487

1.8	1.7781	**0.9**	0.9802	-0.7222	1.6591
1.2	1.1732	**0.6**	0.6562	-0.5065	0.9910
0.6	0.5703	**0.3**	0.3043	-0.8806	0.0745
0.4	0.3866	**0.2**	0.2058	-0.4583	0.3072
0.2	#DIV/0!	**0.1**	#DIV/0!	#DIV/0!	#DIV/0!
			Average Absolute SDI	**0.3634**	**0.7939**

ZY					
Single-Material					
Nominal Length (mm)	**Measured Length (mm)**	**Nominal Width (mm)**	**Measured Width (mm)**	**SD Index Length**	**SD Index Width**
6	6.0779	**3**	2.9906	0.7568	-0.0583
5.4	5.3680	**2.7**	2.6289	-0.3548	-0.7575
4.8	4.8721	**2.4**	2.3955	1.0809	-0.0475
4.2	4.2104	**2.1**	2.0842	0.1399	-0.1325
3.6	3.6238	**1.8**	1.7698	0.4989	-0.3913
3	3.0108	**1.5**	1.4659	0.1404	-0.9699
2.4	2.4051	**1.2**	1.1740	0.0800	-0.8194
1.8	1.7175	**0.9**	0.9464	-0.3053	0.4839
1.2	1.2305	**0.6**	0.4973	0.0965	-1.1953
0.6	0.5208	**0.3**	0.2762	#DIV/0!	#DIV/0!
0.4	#DIV/0!	**0.2**	#DIV/0!	#DIV/0!	#DIV/0!
0.2	#DIV/0!	**0.1**	#DIV/0!	#DIV/0!	#DIV/0!
			Average Absolute SDI	**0.3837**	**0.5395**

Table 17: Error percentage of average measured values for Circular features in both orientations

Circles XY		Circles ZY	
% ERR Multi	**% ERR Single**	**% ERR Multi**	**% ERR Single**
2.2979	5.1194	0.8618	1.6547
2.2384	2.3431	0.1273	1.2560
1.2367	5.1559	1.6548	2.2865
1.8183	4.8523	1.0503	0.7051
6.2843	8.3459	1.4693	2.1095
4.4343	0.2019	5.1962	6.9778
6.2171	3.0719	3.5400	5.5981
6.3571	1.5799	1.4839	2.6909
6.4810	17.4506	0.7929	11.7931
3.9000	7.5794	5.3700	7.2088
NA	NA	7.6500	33.9526
AVERAGE			
4.1265	**5.5700**	**2.6542**	**6.9303**

Table 18: Error percentage of average measured values for rectangular features built in the XY orientation

XY Rectangles			
ERR % L Multi	**ERR % W Multi**	**ERR % L Single**	**ERR % W Single**
1.174	0.124	1.582	5.250
0.408	2.655	0.068	1.836
0.182	0.562	0.641	0.584
0.024	1.038	1.083	3.810
1.234	2.002	0.860	2.506
1.332	2.152	1.030	2.583
0.106	3.921	0.939	0.744
2.821	9.539	1.138	5.135
1.940	17.123	2.728	12.837
0.319	20.129	12.083	3.017
1.950	35.400	NA	NA
NA	NA	NA	NA
AVERAGE			
1.045	**8.604**	**2.215**	**3.830**

Table 19: Error percentage of average measured values for rectangular features built in the Z orientation

ZY Rectangles			
ERR % L Multi	**ERR % W Multi**	**ERR % L Single**	**ERR % W Single**
0.3467	5.3013	1.2989	0.3147
0.6581	0.0241	0.5924	2.6333
0.3190	5.4408	1.5017	0.1868
0.4131	6.5119	0.2484	0.7520
0.8578	1.9122	0.6606	1.6755
0.8437	2.1907	0.3583	2.2711
0.2954	2.3858	0.2108	2.1674
1.3028	8.0233	4.5856	5.1593
0.7492	6.5550	2.5424	17.1125
3.1883	3.8567	13.2000	7.9333
3.3417	2.9000	NA	NA
NA	NA	NA	NA
AVERAGE			
1.1196	**4.1002**	**2.5199**	**4.0206**

References

[1] A. C. Tenhoff, V. Aggarwal, R. Ameduri, A. Deakyne, T. L. Iles, S. M. Said, M. Griselli, and P. A. Iaizzo, "Patient-specific three-dimensional computational heart modeling and printing to enhance clinical understandings and treatment planning: Congenital recurrent pulmonary artery stenosis and transcatheter pulmonary valve replacement," *2021 Design of Medical Devices Conference*, 2021.

[2] Figure 1," in "Patient-specific three-dimensional computational heart modeling and printing to enhance clinical understandings and treatment planning: Congenital recurrent pulmonary artery stenosis and transcatheter pulmonary valve replacement," *Design of Medical Devices Conference,* 2021.

[3] Bourell, D. L., Rosen, D. W., & Leu, M. C. (2014). The roadmap for additive manufacturing and its impact. *3D Printing and Additive Manufacturing*, 1(1), 6-9.

[4] Witherell P, Herron J, Ameta G (2016) Towards Annotations and Product Definitions for Additive Manufacturing. Procedia. CIRP 43:339–344. doi: 10.1016/j.procir.2016.01.198

[5] "What is MBD?: Model-based definition," PTC. [Online]. Available: https://www.ptc.com/en/technologies/cad/model-based-definition. [Accessed: 06-Feb-2023].

[6] T. Hedberg, J. Lubell, L. Fischer, L. Maggiano, and A. Barnard Feeney, "Testing the digital thread in support of model-based manufacturing and Inspection," *Journal of Computing and Information Science in Engineering*, vol. 16, no. 2, 2016.

[7] J. Allison, C. Sharpe, and C. C. Seepersad, "A test part for evaluating the accuracy and resolution of a polymer powder bed fusion process," *Journal of Mechanical Design*, vol. 139, no. 10, 2017.

[8] N. Meisel and C. Williams, "An investigation of key design for additive manufacturing constraints in multimaterial three-dimensional printing," *Journal of Mechanical Design*, vol. 137, no. 11, 2015.

[9] D. W. Rosen, "Research supporting principles for design for Additive Manufacturing," *Virtual and Physical Prototyping*, vol. 9, no. 4, pp. 225–232, 2014

[10] L. L. Lopez Taborda, H. Maury, and J. Pacheco, "Design for Additive Manufacturing: A comprehensive review of the tendencies and limitations of methodologies," *Rapid Prototyping Journal*, vol. 27, no. 5, pp. 918–966, 2021.

[11] T. W. Simpson, "Additive manufacturing standards," Additive Manufacturing, 22-Jun-2021. [Online]. Available: https://www.additivemanufacturing.media/articles/standards-for-additive-manufacturing. [Accessed: 18-Jul-2022]

[12] A. Cazón, P. Morer, and L. Matey, "PolyJet technology for product prototyping: Tensile strength and surface roughness properties," *Proceedings of the Institution of Mechanical Engineers, Part B: Journal of Engineering Manufacture*, vol. 228, no. 12, pp. 1664–1675, 2014.

[13] Y. L. Yap, C. Wang, S. L. Sing, V. Dikshit, W. Y. Yeong, and J. Wei, "Material Jetting Additive Manufacturing: An experimental study using designed metrological benchmarks," *Precision Engineering*, vol. 50, pp. 275–285, 2017.z

[14] R. Udroiu, I. Braga, and A. Nedelcu, "Evaluating the quality surface performance of additive manufacturing systems: Methodology and a material jetting case study," *Materials*, vol. 12, no. 6, p. 995, 2019.

[15] R. K. Leach, D. Bourell, S. Carmignato, A. Donmez, N. Senin, and W. Dewulf, "Geometrical metrology for Metal Additive Manufacturing," *CIRP Annals*, vol. 68, no. 2, pp. 677–700, 2019.

[16] L. Rebaioli and I. Fassi, "A review on benchmark artifacts for evaluating the geometrical performance of additive manufacturing processes," *The International Journal of Advanced Manufacturing Technology*, vol. 93, no. 5-8, pp. 2571–2598, 2017.

[17] A. K. Sood, R. K. Ohdar, and S. S. Mahapatra, "Parametric appraisal of mechanical property of fused deposition modelling processed parts," *Materials & Design*, vol. 31, no. 1, pp. 287–295, Jun. 2009.

[18] M. Braian, R. Jimbo, and A. Wennerberg, "Production tolerance of additive manufactured polymeric objects for clinical applications," *Dental Materials*, vol. 32, no. 7, pp. 853–861, Mar. 2016.

[19] Y. L. Tee, P. Tran, M. Leary, P. Pille, and M. Brandt, "3D printing of polymer composites with material jetting: Mechanical and fractographic analysis," *Additive Manufacturing*, vol. 36, p. 101558, Aug. 2020.

[20] Yap, Y. L., Wang, C., Tan, H., Dikshit, V., and Yeong, W. Y., 2016, "Benchmarking Of Material Jetting Process: Process Capability Study."

[21] Mendricky, R., 2016, "Accuracy Analysis of Additive Technique for Parts Manufacturing," *MM Science Journal*, 2016(05), pp. 1502-1508.

[22] N. J. Kent, L. Jolivet, P. O'Neill, and D. Brabazon, "An evaluation of components manufactured from a range of materials, fabricated using PolyJet technology," *Advances in Materials and Processing Technologies*, vol. 3, no. 3, pp. 318–329, 2017.

[23] K. Thakare, X. Wei, and Z. Pei, "Dimensional Accuracy in PolyJet printing: A literature review," *Volume 1: Additive Manufacturing; Manufacturing Equipment and Systems; Bio and Sustainable Manufacturing*, Jun. 2019.

[24] *SUP706B*. Stratasys. (n.d.). Retrieved November 12, 2022, from https://www.stratasys.com/en/materials/materials-catalog/polyjet-materials/polyjet-support-materials/sup706B/

[25] "Stratasys J735 & J750 multi-material, professional 3D printer," Proto3000, 22-Nov-2022. [Online]. Available: https://proto3000.com/product/stratasys-j750/#specs. [Accessed: 12-Mar-2023].

[26] A. Nahum, "Matte or glossy? which finish to use for your 3D prints and when.," Matte or Glossy? Which Finish to Use for Your 3D Prints and When. | GrabCAD Tutorials, 10-Jan-2019. [Online]. Available: https://grabcad.com/tutorials/matte-or-glossy-which-finish-to-use-for-your-3d-prints-and-when. [Accessed: 10-Feb-2022].

[27] C. C. Seepersad, T. Govett, K. Kim, M. Lundin, and D. Pinero, "A designer's guide for dimensioning and tolerancing SLS parts," *TexasScholarWorks*, 2012. [Online]. Available: http://dx.doi.org/10.26153/tsw/15400. [Accessed: 10-Jan-2022].

[28] Thresholding. ImageJ Wiki. (n.d.). Retrieved March 28, 2023, from https://imagej.net/imaging/thresholding

[29] Department of Defense. "MIL-STD-31000A Standard Practice: Technical Data Packages", Feb. 2013.